3 1176 00005 6953

JAN 31 1947

NACA 65-210/5

NATIONAL ADVISORY COMMITTEE FOR AERONAUTICS

TECHNICAL NOTE

No. 1167

PRESSURE DISTRIBUTIONS AND FORCE TESTS OF AN NACA 65-210 AIRFOIL SECTION WITH A 50-PERCENT-CHORD FLAP

By Milton M. Klein

Langley Memorial Aeronautical Laboratory
Langley Field, Va.

Washington
January 1947

NACA LIBRARY
LANGLEY MEMORIAL AERONAUTICAL
LABORATORY
Langley Field, Va.

NATIONAL ADVISORY COMMITTEE FOR AERONAUTICS

TECHNICAL NOTE NO. 1167

PRESSURE DISTRIBUTIONS AND FORCE TESTS OF AN NACA 65-210 AIRFOIL SECTION WITH A 50-PERCENT-CHORD FLAP

By Milton M. Klein

SUMMARY

Pressure distributions and force measurements were made in the Langley two-dimensional low-turbulence pressure tunnel at low Mach numbers and high Reynolds numbers of an NACA 65-210 airfoil equipped with a 50-percent-chord plain flap. The tests were carried out for flap deflections of 0°, 4°, 7°, and 10°. The data showed that these flap deflections provided considerably reduced drag coefficients at lift coefficients above the design range of the plain airfoil. The variations of maximum lift, minimum drag, and pitching moment at minimum drag with flap deflection were nearly linear, within the range of flap deflections tested. The measured increments of the pitching moment and of the angle of zero lift resulting from flap deflection compared satisfactorily with those calculated from thin-airfoil theory.

INTRODUCTION

Force coefficients and chordwise pressure distributions obtained in high Reynolds number and low Mach number tests of an NACA 65-210 airfoil equipped with a 50-percent-chord flap are presented. The original purpose of the work was to investigate the following two problems:

(1) The possibility of increasing the critical Mach numbers of thin airfoils at lift coefficients above the design range by providing increased camber through the deflection of a large-chord flap.

(2) The possibility that variable camber obtained by flap deflection would permit the attainment of low drags at lift coefficients above the normal airfoil design range.

In view of the rapid decrease of the critical Mach numbers of thin airfoils outside the design range, which is predicted in the supplementary figures of reference 1, it appears important to investigate the possibility of increasing the critical Mach numbers of thin airfoils at lift coefficients above the design range. Recent high-speed work (unpublished data from Ames Aeronautical Laboratory) has indicated, however, that above the design lift range low-speed data do not suffice to permit prediction of the Mach number at which critical compressibility effects occur.

Accordingly, the significance of the first problem appears at present to be somewhat uncertain. The measured pressure distributions and their correlation with thin-airfoil theory, however, appear of considerable interest; the drag results are also of interest with regard to the attainment of low drags at lift coefficients above the design range of the plain airfoil.

The tests were made in the Langley two-dimensional low-turbulence pressure tunnel.

SYMBOLS

c	airfoil chord
c_d	section drag coefficient
c_l	section lift coefficient
$c_{m_{a.c.}}$	section pitching-moment coefficient about aerodynamic center
$c_{m_{c/4}}$	section pitching-moment coefficient about quarter-chord point
H_o	free-stream total pressure
M_{cr}	critical Mach number
p	local static pressure
q_o	free-stream dynamic pressure
R	Reynolds number

S pressure coefficient $\left(\frac{H_o - p}{q_o}\right)$

x distance along chord measured from leading edge

y distance perpendicular to chord line measured from chord line

α_o section angle of attack

α_{l_o} angle of zero lift

δ_f flap deflection

Subscripts:

max maximum

min minimum

MODELS AND TESTS

The models used in the present tests were made of mahogany laminated in the spanwise direction. Four models, each having a chord of 24 inches, were made with flap deflections of 0°, 4°, 7°, and 10°. The flap deflections were obtained by rotating the rearward half of the airfoil about the point on the lower surface at the 50-percent chordwise position. Ordinates for the undeflected airfoil are given in table I, and the method of deflection is shown in the sketch above the table. The method of testing was the same as that described in reference 1 for 2-foot-chord models in the Langley two-dimensional low-turbulence pressure tunnel.

Lift, drag, and pitching moment were obtained for the flap-neutral condition at Reynolds numbers of 3.0×10^6, 6.0×10^6, and 9.0×10^6 and for the various flap deflections at a Reynolds number of 6.0×10^6. Lift and drag with standard roughness applied to the leading edge were obtained for flap deflections of 0°, 4°, and 7° at a Reynolds number of 6.0×10^6. Pressure distributions were obtained for all the flap deflections at a Reynolds number of 6.0×10^6 for a range of angle of attack from moderate negative values to beyond the positive stall. The highest Mach number encountered during the tests was less than 0.15.

Corrections for the effects of wind-tunnel wall interference upon the angle of attack and the aerodynamic coefficients were made by the methods described in the appendix of reference 1. The magnitude of the corrections was of the order of only a few percent.

RESULTS AND DISCUSSION

The lift, drag, and pitching-moment characteristics for flap deflections of 0°, 4°, 7°, and 10° of the NACA 65-210 airfoil section are presented in figures 1 to 4, respectively. The corresponding pressure distributions are shown in figures 5 to 8. The pressure distributions for the various flap deflections, as expected, show peaks on the upper and lower surfaces near the 50-percent chordwise position where the direction of the surface changes rapidly. The lift coefficients at which a pressure peak first appears at the nose are increased by flap deflection.

The variations with flap deflection of section maximum lift coefficient, section minimum drag coefficient, and section pitching-moment coefficient at minimum drag are shown in figure 9 for a Reynolds number of 6.0×10^6. The variations of these coefficients with flap deflection are nearly linear. A flap deflection of 10° increases the maximum lift coefficient from 1.33 to 1.59, increases the minimum drag coefficient from 0.0038 to 0.0056, and negatively increases the pitching-moment coefficient from -0.035 to -0.122.

As has already been implied, the critical Mach number that is obtained from low-speed pressure distributions does not define the break in the curve of lift coefficient against Mach number for a given angle of attack. Actually, outside the design range the break may occur at Mach numbers considerably higher than the predicted critical Mach number (as shown by unpublished data from Ames Aeronautical Laboratory). For the sake of completeness, however, curves of predicted critical Mach number against low-speed section lift coefficient (computed by means of the critical Mach number chart of reference 1, p. S83) are presented in figure 10. The envelope curve, also drawn in figure 10, shows that the small flap deflections provide large increases in the predicted critical Mach numbers at moderately high lift coefficients.

The drag curves of figures 1 to 4 for a Reynolds number of 6.0×10^6 are plotted together in figure 11 along with their envelope. Figure 11 shows the lowest drag coefficients obtainable for the flapped airfoil as a function of lift coefficient. The highest lift coefficient for which a low drag coefficient was obtained was 0.76

at $\delta_f = 10^\circ$. The corresponding drag coefficient, 0.0059, was much less than that of the plain airfoil at the same lift coefficient but was appreciably higher than the drag coefficients measured on airfoils designed for the higher lift range.

In order to check the validity of thin-airfoil theory for large-chord flaps, a comparison is presented in the following table of the experimental and calculated increments, due to flap deflection, of the angle of zero lift and the pitching moment about the quarter chord point:

δ_f (deg)	Calculated $\Delta\alpha_{l_o}$ (deg)	Experimental $\Delta\alpha_{l_o}$ (deg)	Calculated $\Delta c_{m_{c/4}}$	Experimental $\Delta c_{m_{c/4}}$
4	3.28	2.90	-0.035	-0.040
7	5.73	5.90	-.061	-.067
10	8.17	7.90	-.087	-.087

The calculated values in this table were obtained by the method of reference 2. The table indicates that for a large-chord flap reasonably accurate values of the angle of zero lift and of the pitching-moment coefficient may be obtained from thin-airfoil theory.

CONCLUSIONS

Pressure distributions and force measurements at low Mach numbers and high Reynolds numbers on an NACA 65-210 airfoil with a 50-percent-chord flap deflected 0°, 4°, 7°, and 10° indicated the following conclusions:

(1) Considerable reduction of the drag coefficients above the low-drag range of the plain airfoil may be effected by use of small deflections of a large-chord flap.

(2) The variations of maximum lift, minimum drag, and pitching moment at minimum drag with flap deflection were nearly linear within the range of flap deflections tested.

(3) Reasonably accurate values of the angle of zero lift and the pitching-moment coefficient for airfoils with large-chord flaps may be obtained from thin-airfoil theory.

Langley Memorial Aeronautical Laboratory
National Advisory Committee for Aeronautics
Langley Field, Va., July 8, 1946

REFERENCES

1. Abbott, Ira H., von Doenhoff, Albert E., and Stivers, Louis S., Jr.: Summary of Airfoil Data. NACA ACR No. L5C05, 1945.

2. Glauert, H.: Theoretical Relationships for an Aerofoil with Hinged Flap. R. & M. No. 1095, British A.R.C., 1927.

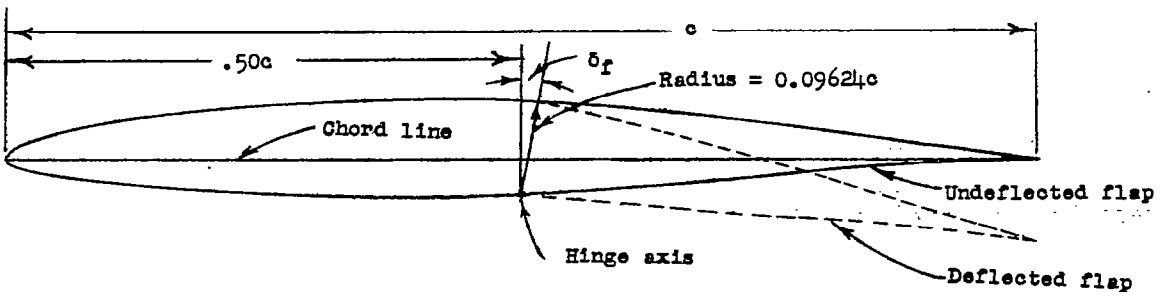

TABLE I.- ORDINATES FOR THE NACA 65-210 AIRFOIL SECTION, $\delta_f = 0°$

[Stations and ordinates given in percent of airfoil chord]

Upper Surface		Lower Surface	
Station	Ordinate	Station	Ordinate
0	0	0	0
.435	.819	.565	-.719
.678	.999	.822	-.859
1.169	1.273	1.331	-1.059
2.408	1.757	2.592	-1.385
4.898	2.491	5.102	-1.859
7.394	3.069	7.606	-2.221
9.894	3.555	10.106	-2.521
14.899	4.338	15.101	-2.992
19.909	4.938	20.091	-3.346
24.921	5.397	25.079	-3.607
29.936	5.732	30.064	-3.788
34.951	5.954	35.049	-3.894
39.968	6.067	40.032	-3.925
44.984	6.058	45.016	-3.868
50.000	5.915	50.000	-3.709
55.014	5.625	54.986	-3.435
60.027	5.217	59.973	-3.075
65.036	4.712	64.964	-2.652
70.043	4.128	69.957	-2.184
75.045	3.479	74.955	-1.689
80.044	2.783	79.956	-1.191
85.038	2.057	84.962	-.711
90.028	1.327	89.972	-.293
95.014	.622	94.986	.010
100.000	0	100.000	0

L.E. radius: 0.687
Slope of radius through L.E.: 0.084

NATIONAL ADVISORY
COMMITTEE FOR AERONAUTICS

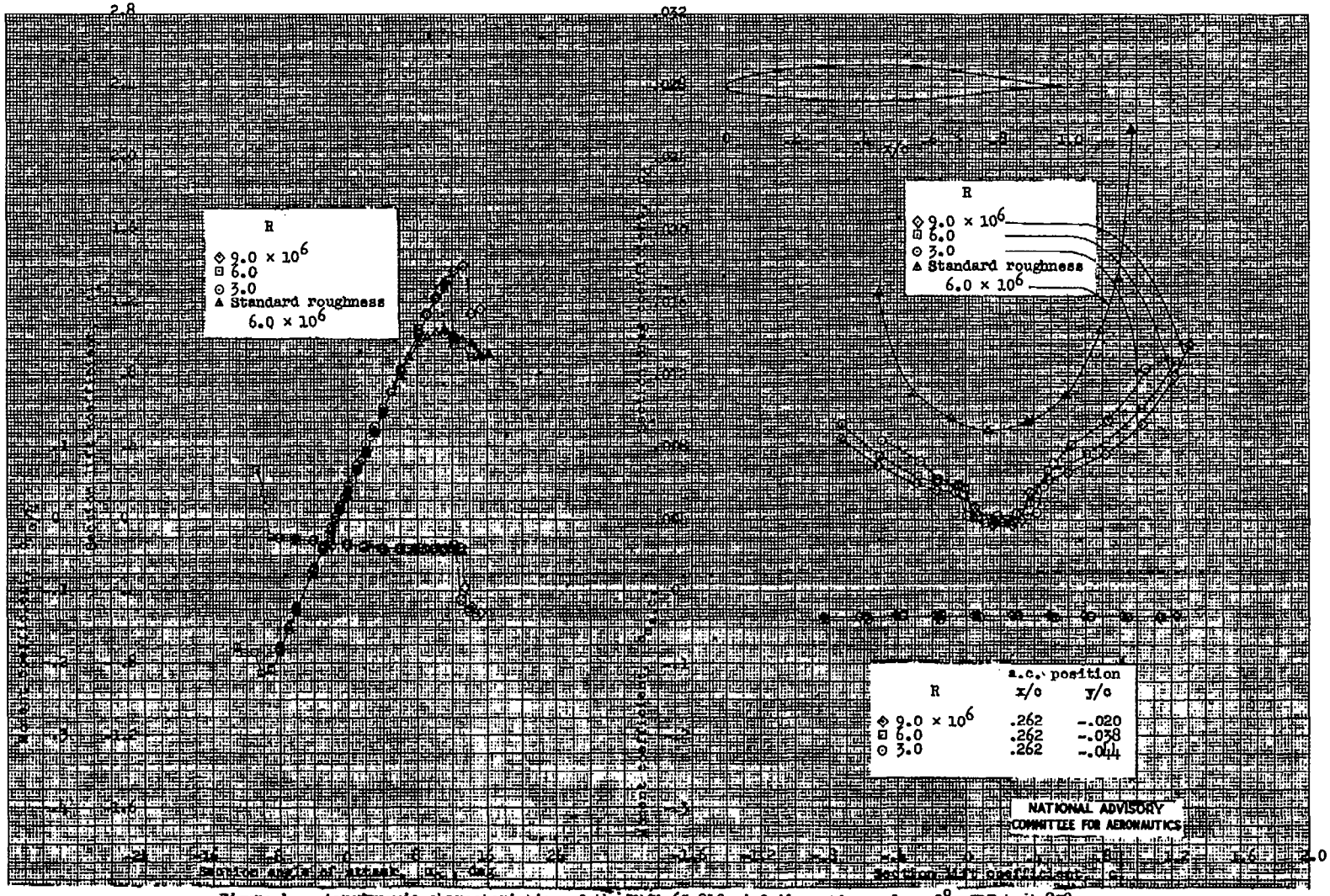

Figure 1.- Aerodynamic characteristics of the NACA 65-210 airfoil section. $\delta_f = 0^\circ$; TDT test 828.

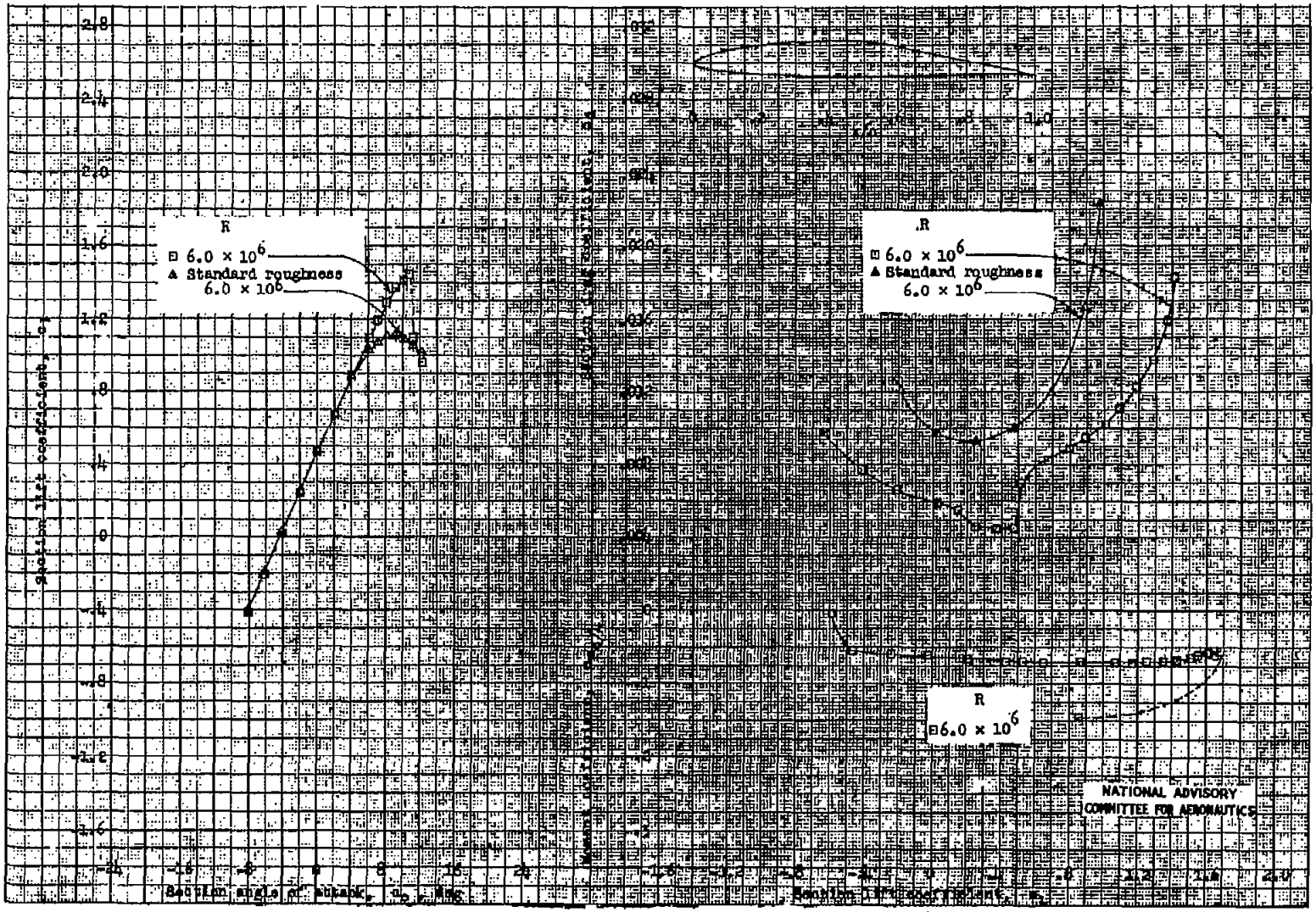

Figure 2.- Aerodynamic characteristics of the NACA 65-210 airfoil section. $\delta_f = 4^\circ$; TDT test 874.

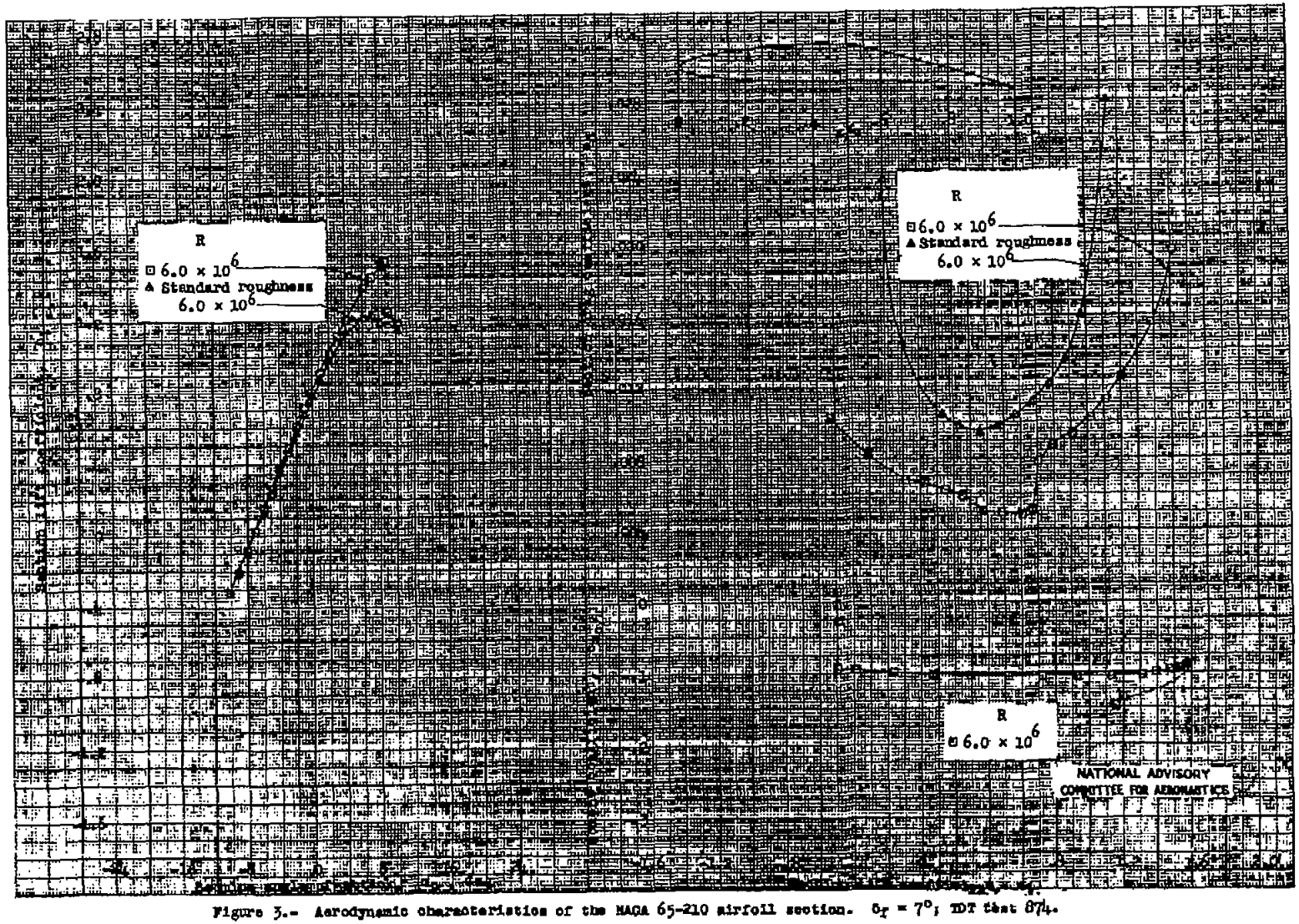

Figure 3.- Aerodynamic characteristics of the NACA 65-210 airfoil section. $\delta_f = 7^\circ$; TDT test 874.

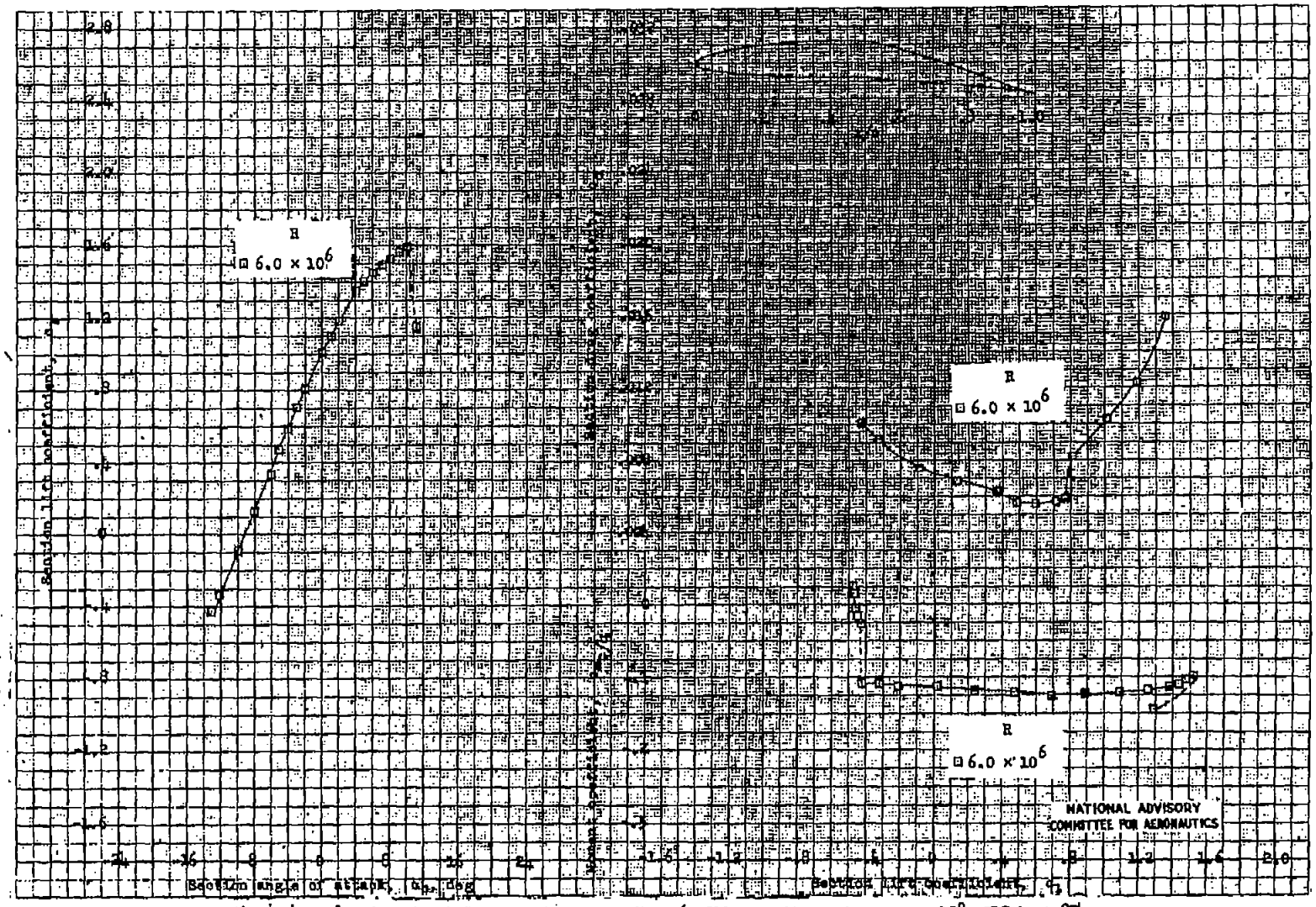

Figure 4.- Aerodynamic characteristics of the NACA 65-210 airfoil section. $\delta_f = 10^\circ$; TDT test 874.

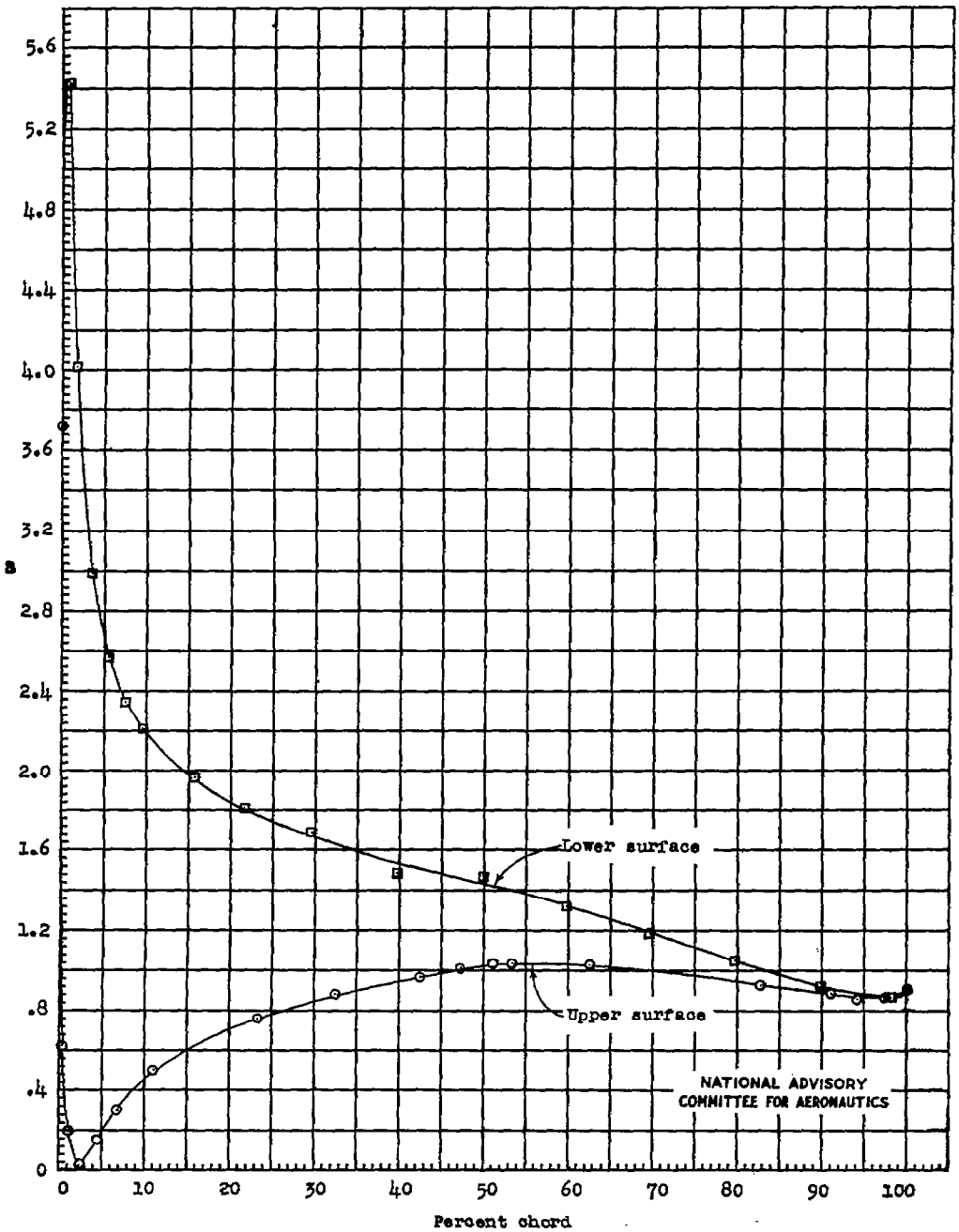

(a) $\alpha_o = -8.12^\circ$

Figure 5.- Pressure distribution for the NACA 65-210 airfoil section. $\delta_f = 0^\circ$; $R = 6.0 \times 10^6$; TDT test 874.

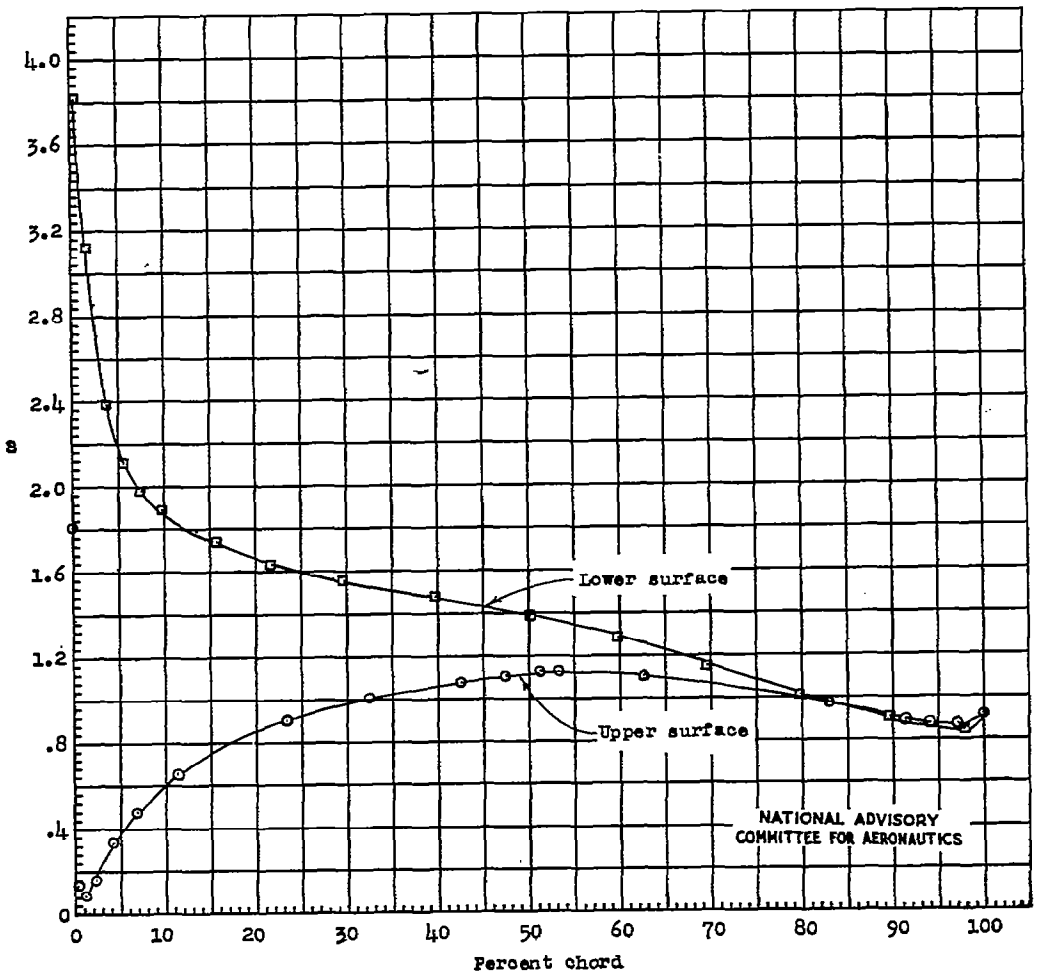

(b) $\alpha_o = -6.09^\circ$

Figure 5.- Continued.

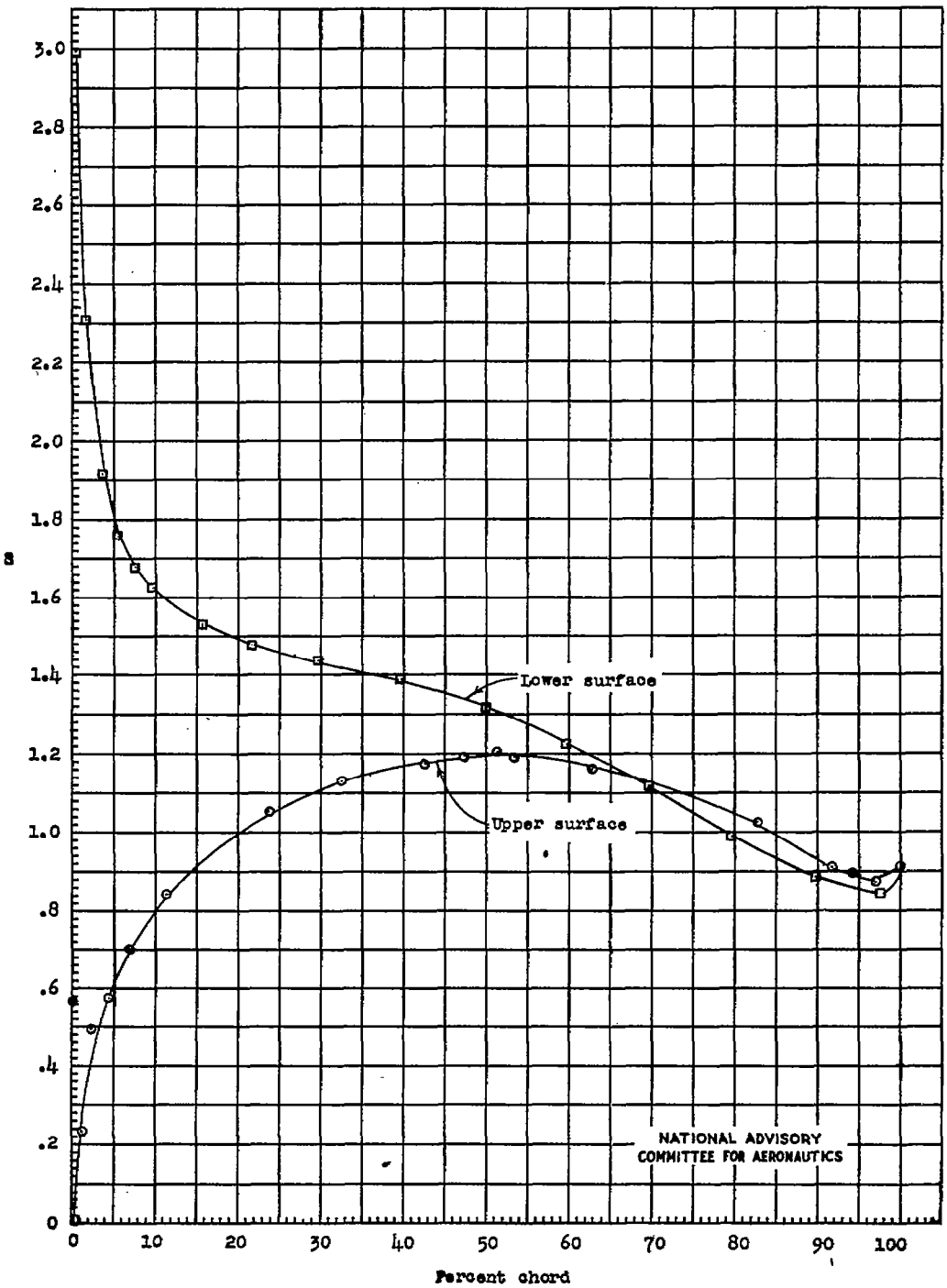

(c) $\alpha_o = -4.06^\circ$

Figure 5.- Continued.

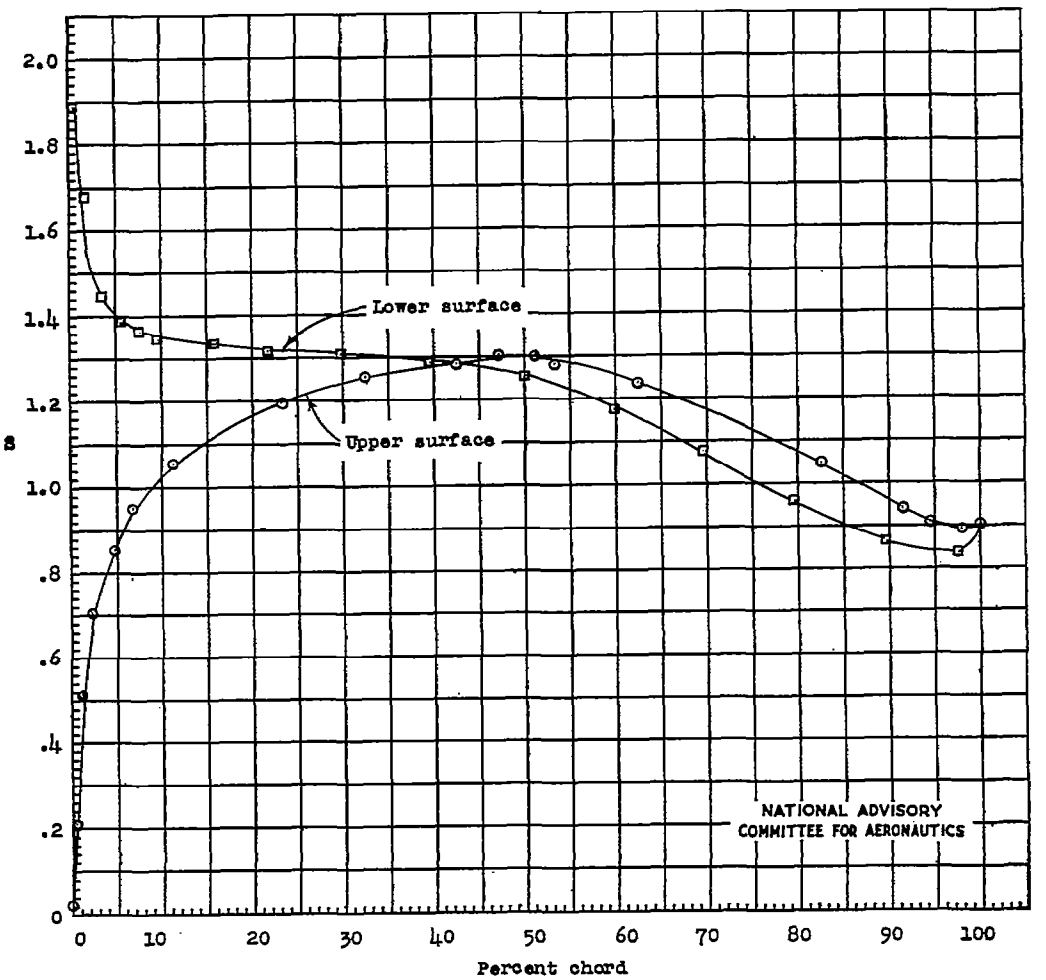

(d) $\alpha_o = -2.03^\circ$.

Figure 5.- Continued.

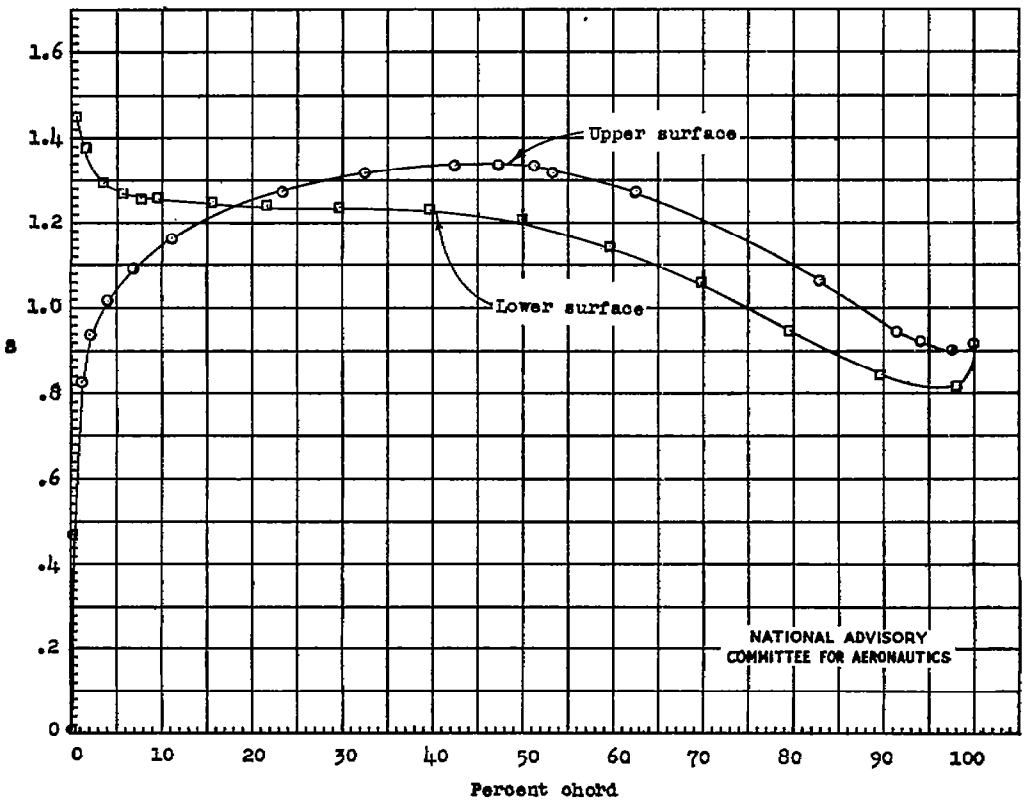

(e) $\alpha_0 = -1.02^\circ$

Figure 5.- Continued.

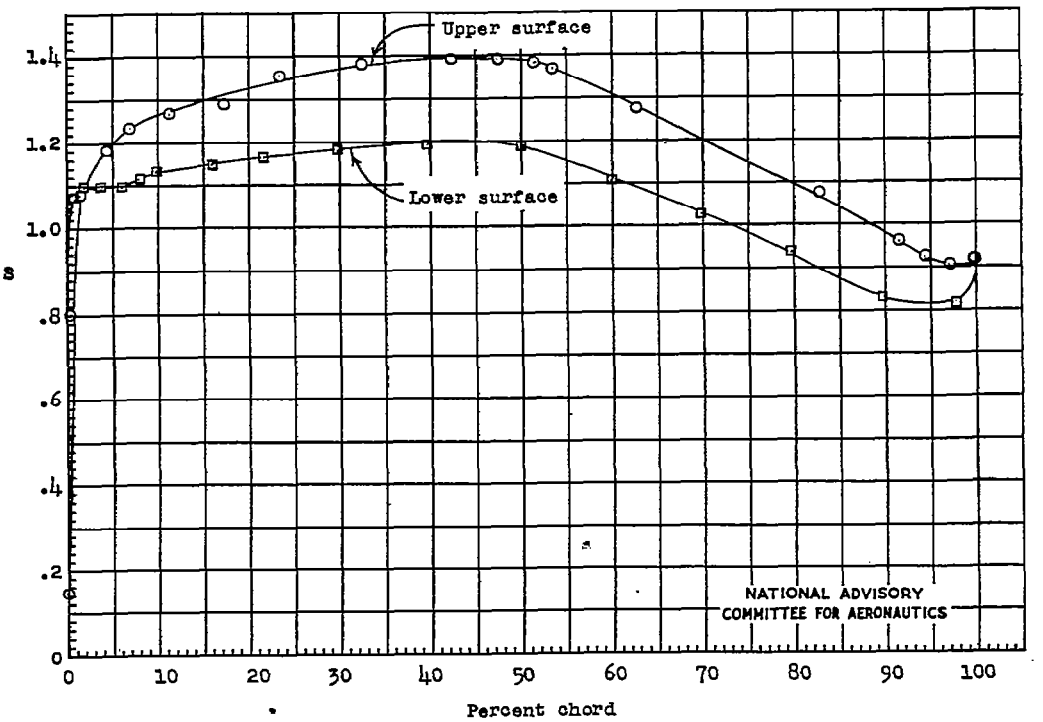

(f) $\alpha_o = 0^\circ$

Figure 5.- Continued.

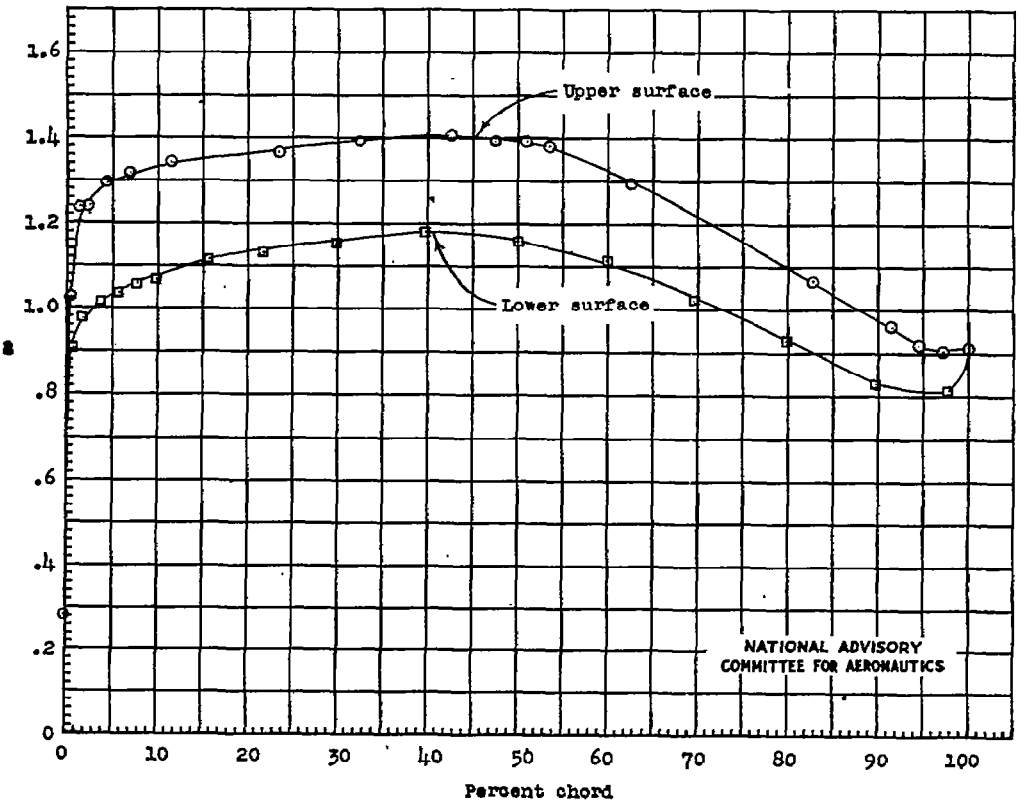

(g) $\alpha_o = 0.51^\circ$.

Figure 5.- Continued.

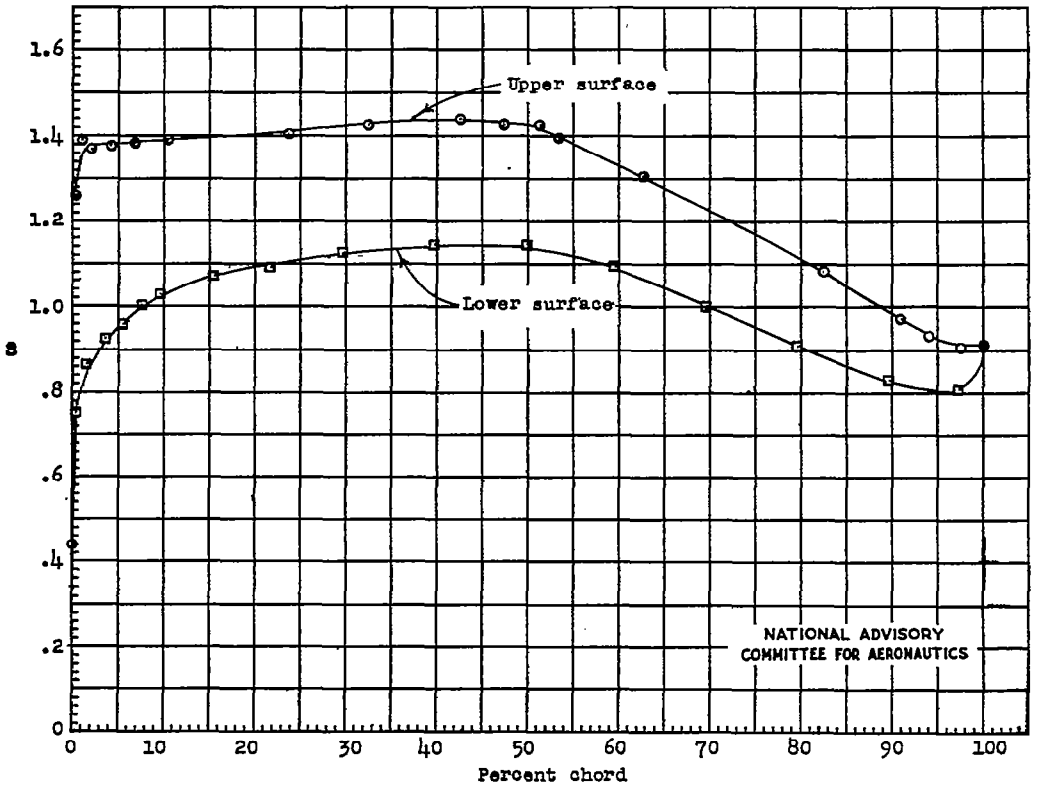

(h) $\alpha_o = 1.02^\circ$.

Figure 5.- Continued.

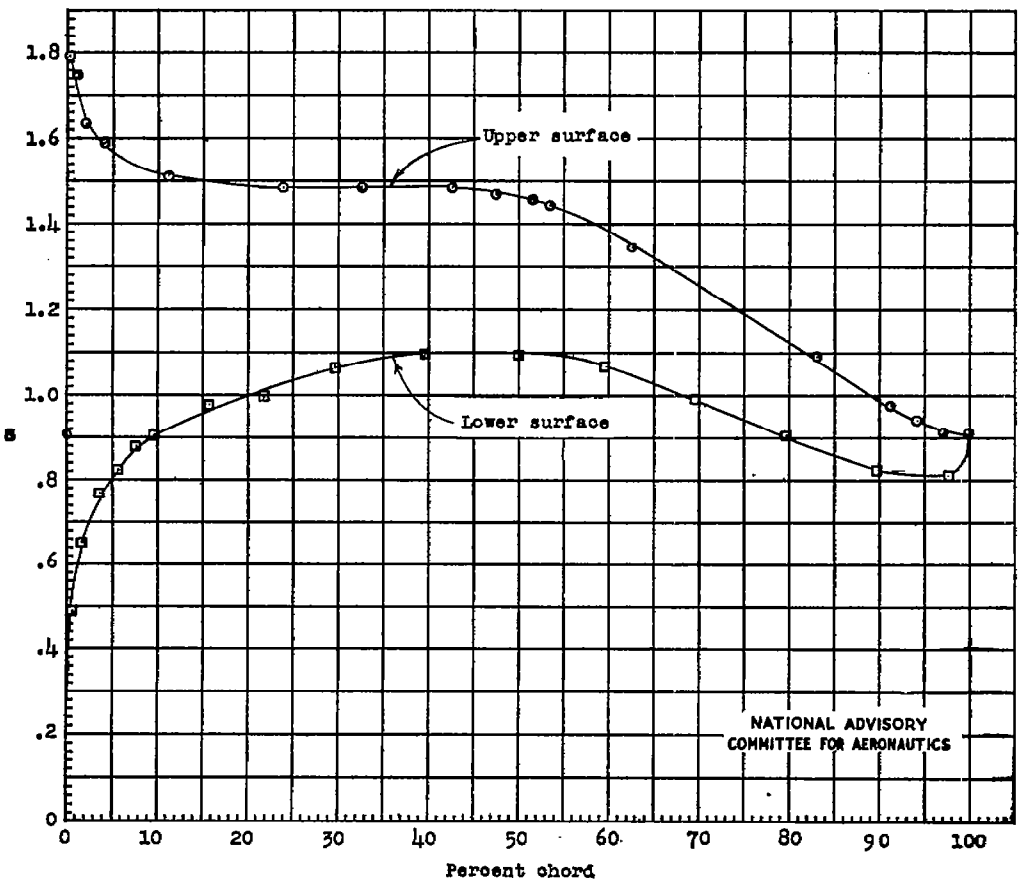

(i) $\alpha_o = 2.03^\circ$.

Figure 5.- Continued.

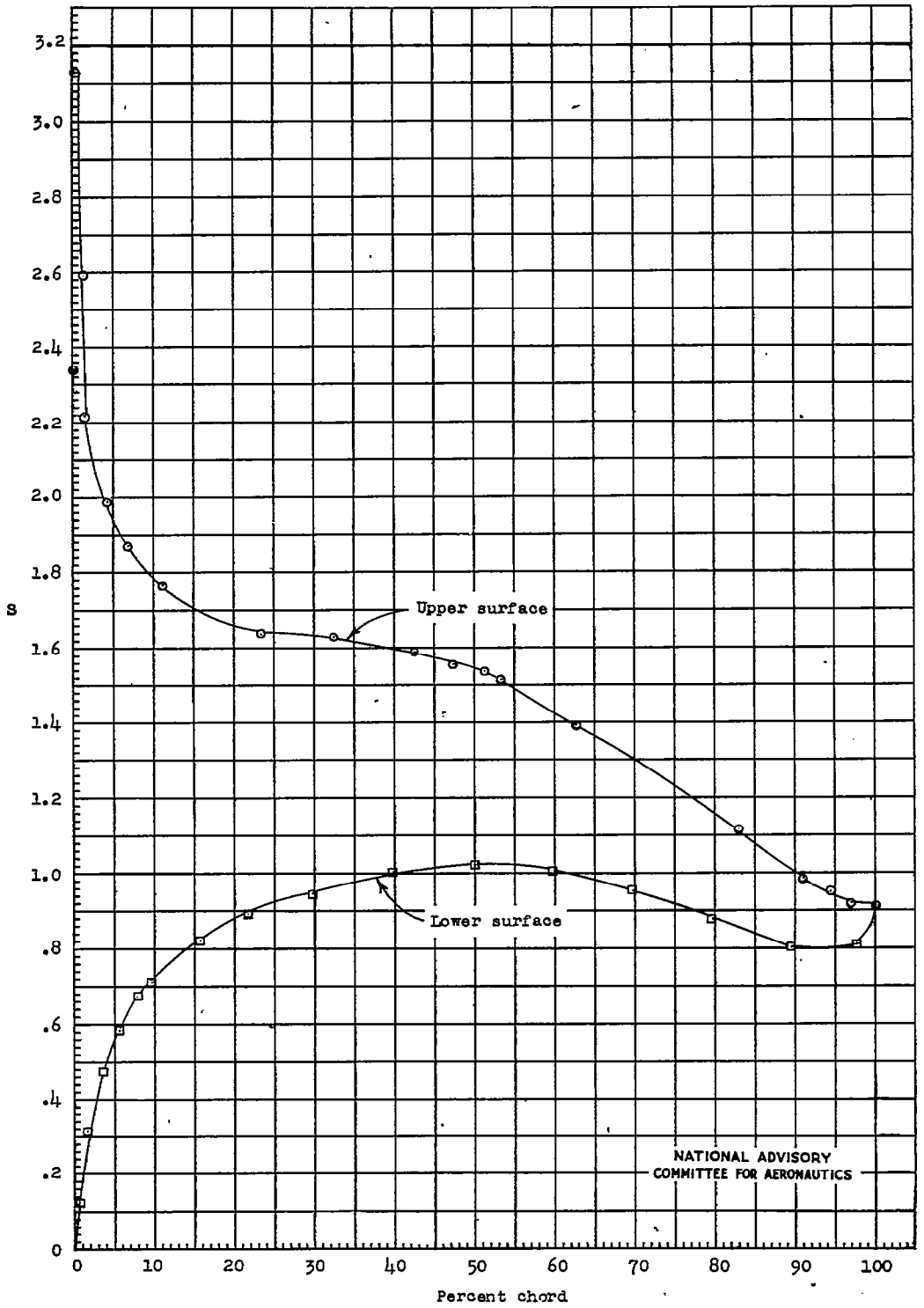

(j) $\alpha_o = 4.06^\circ$

Figure 5.- Continued.

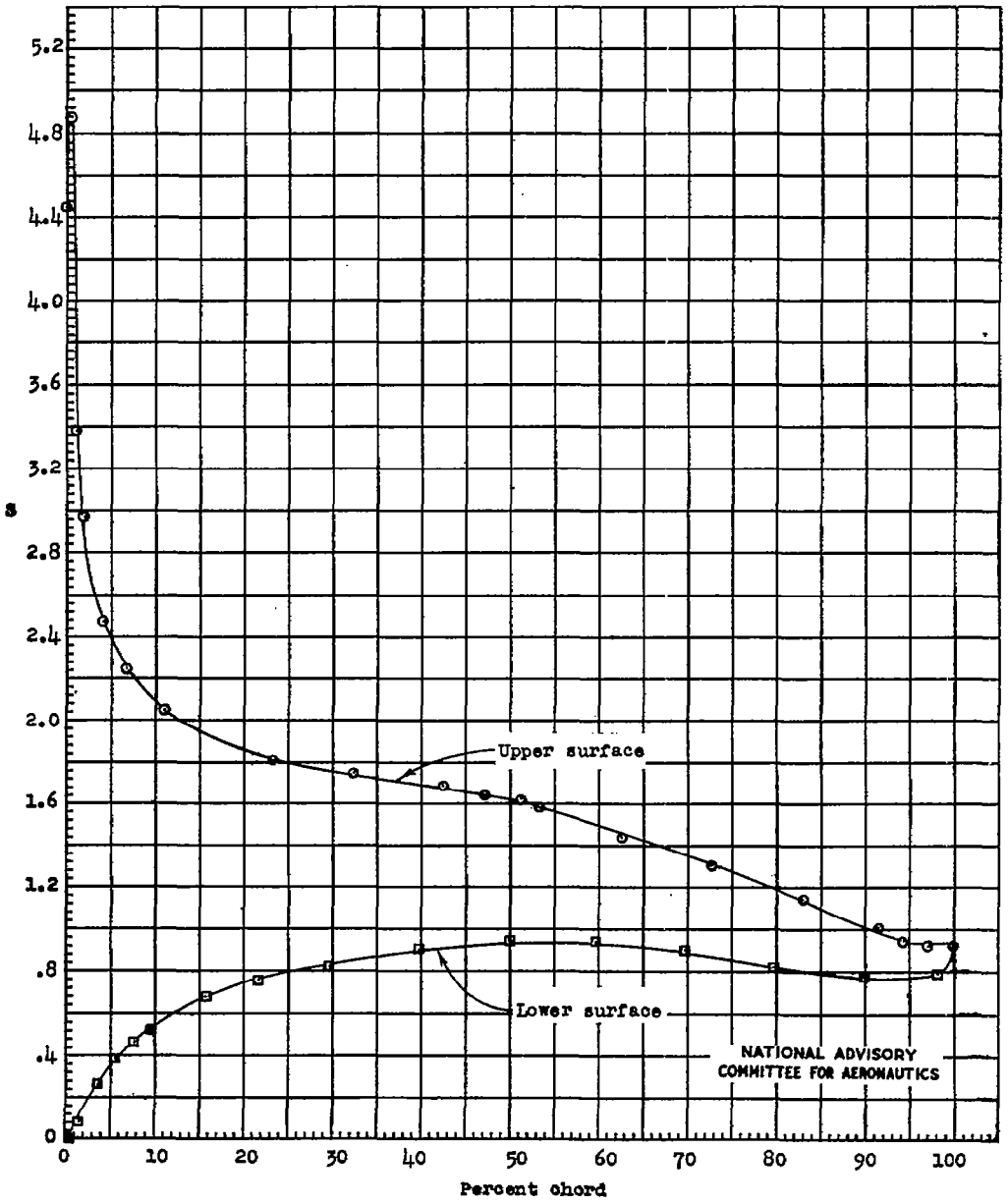

(k) $\alpha_o = 6.09^\circ$

Figure 5.- Continued.

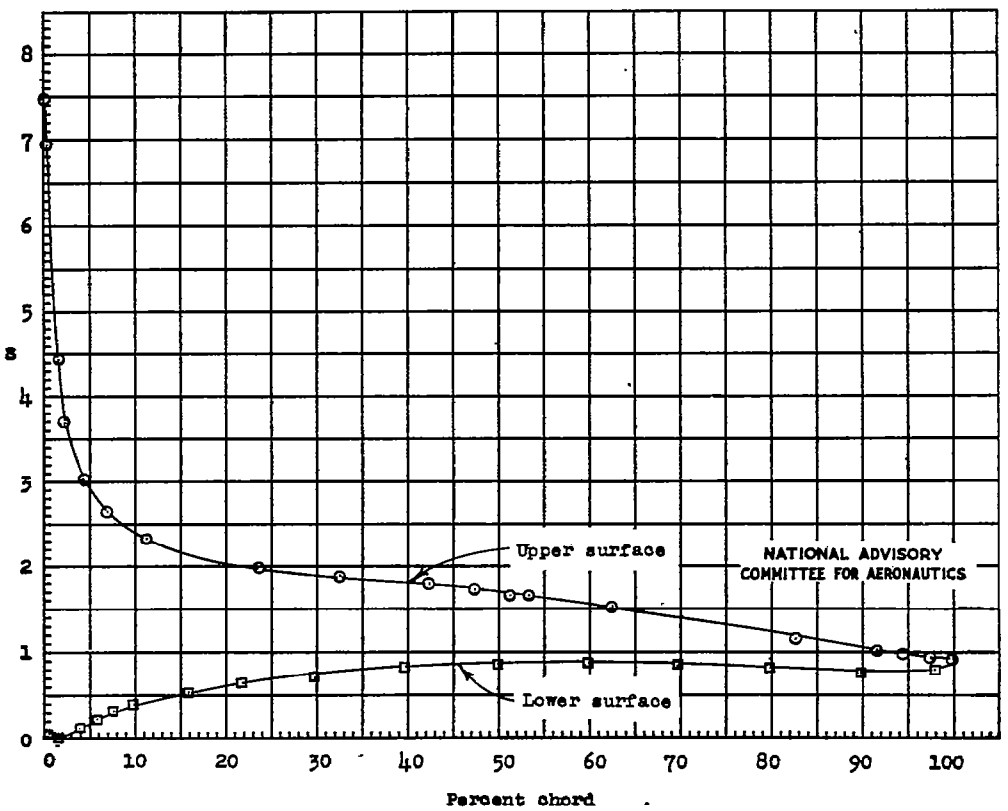

(1) $\alpha_o = 8.12^\circ$

Figure 5.- Continued.

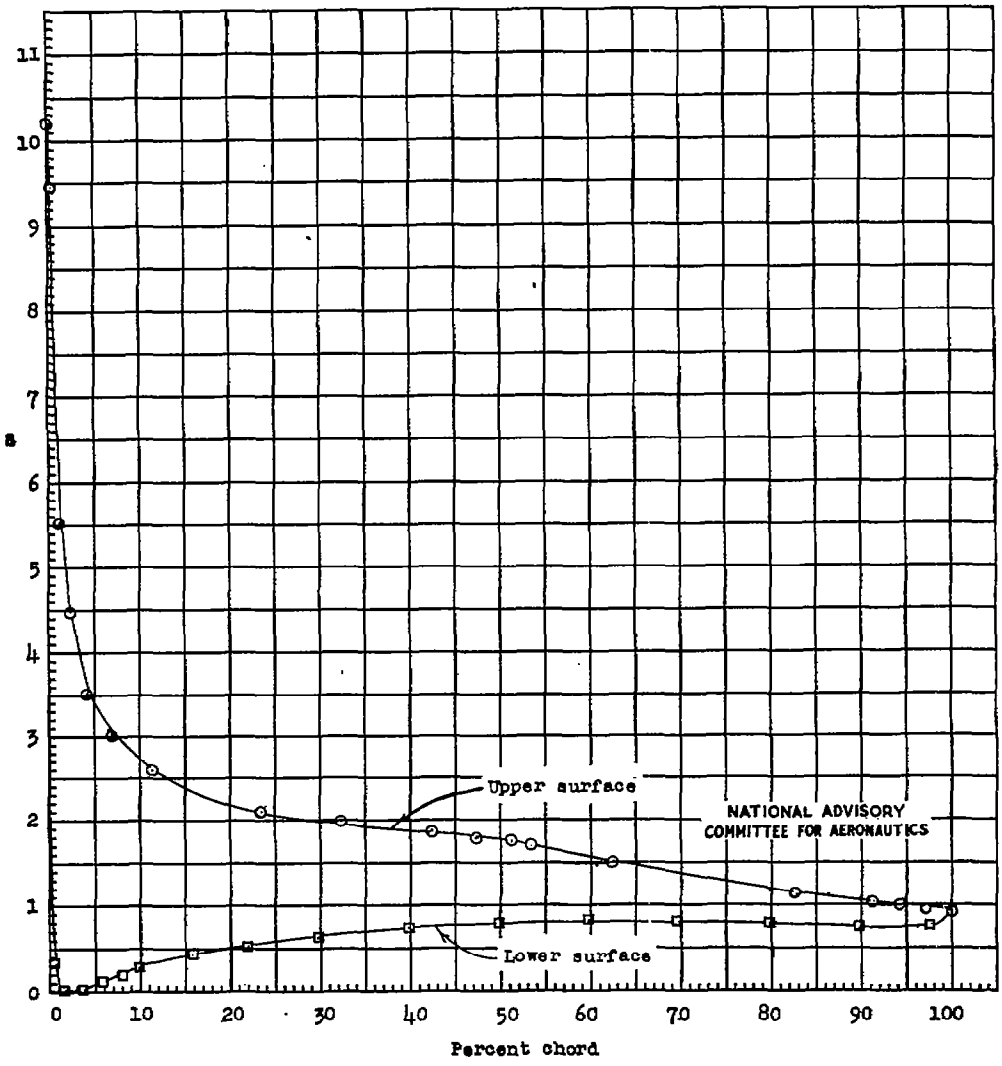

(m) $\alpha_o = 10.15^\circ$

Figure 5.- Continued.

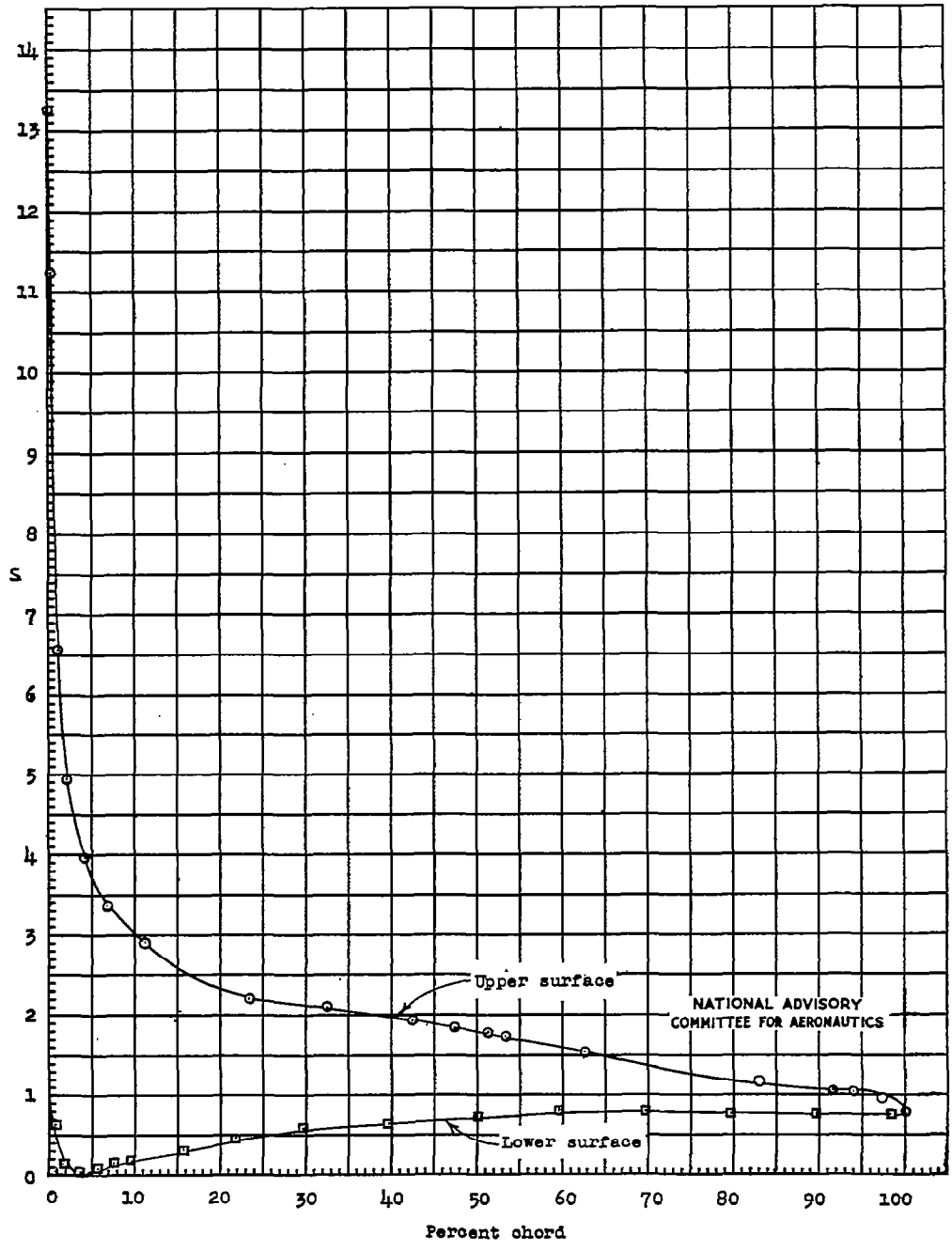

(n) $\alpha_o = 12.18^\circ$

Figure 5.- Concluded.

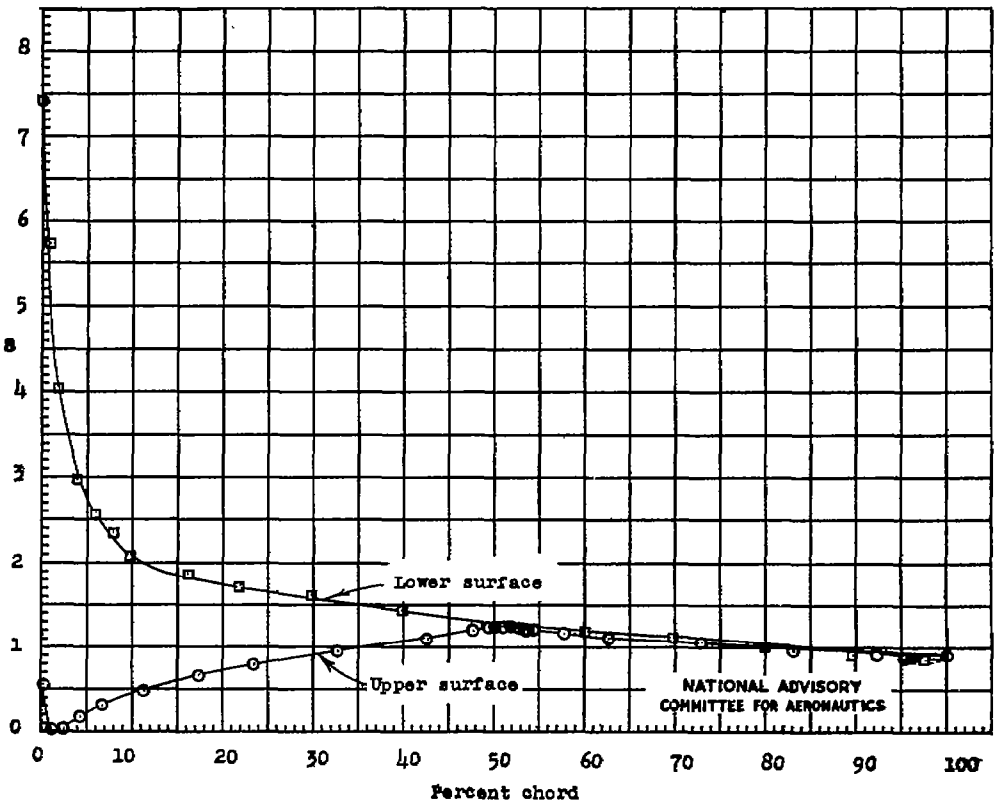

(a) $\alpha_o = -10.15^\circ$

Figure 6.- Pressure distribution for the NACA 65-210 airfoil section. $\delta_f = 4^\circ$; $R = 6.0 \times 10^6$; TDT test 874.

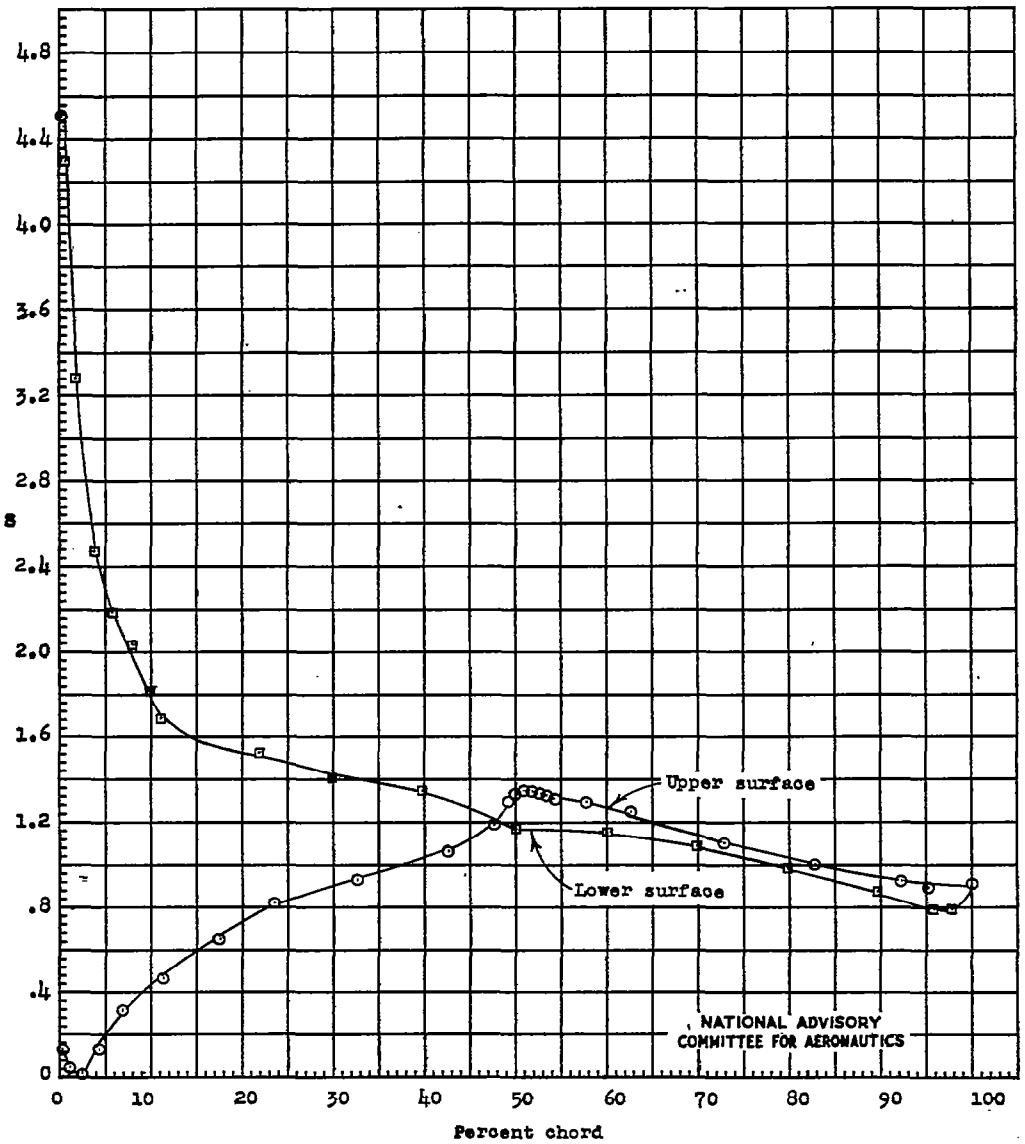

(b) $\alpha_o = -8.12^\circ$

Figure 6.- Continued.

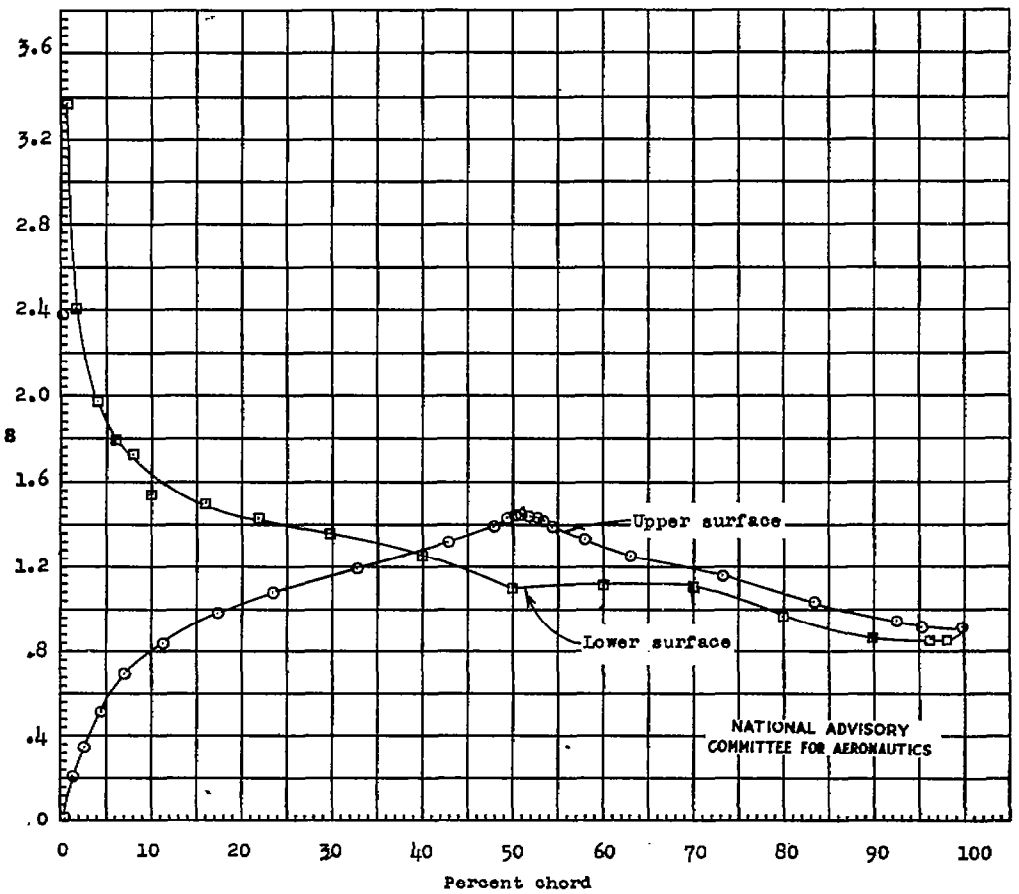

(c) $\alpha_o = -6.09°$

Figure 6.- Continued.

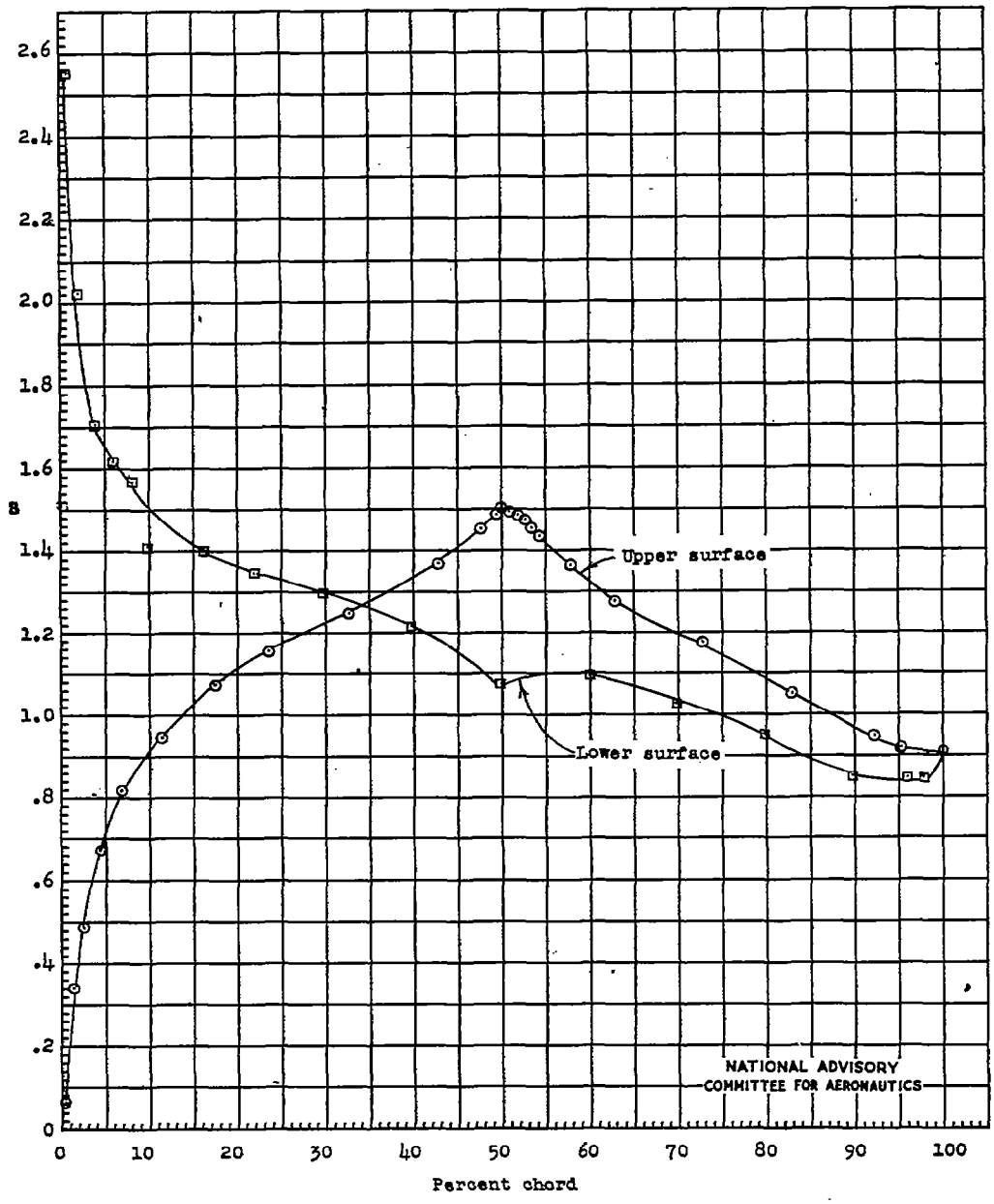

(d) $\alpha_o = -5.08^\circ$.

Figure 6.- Continued.

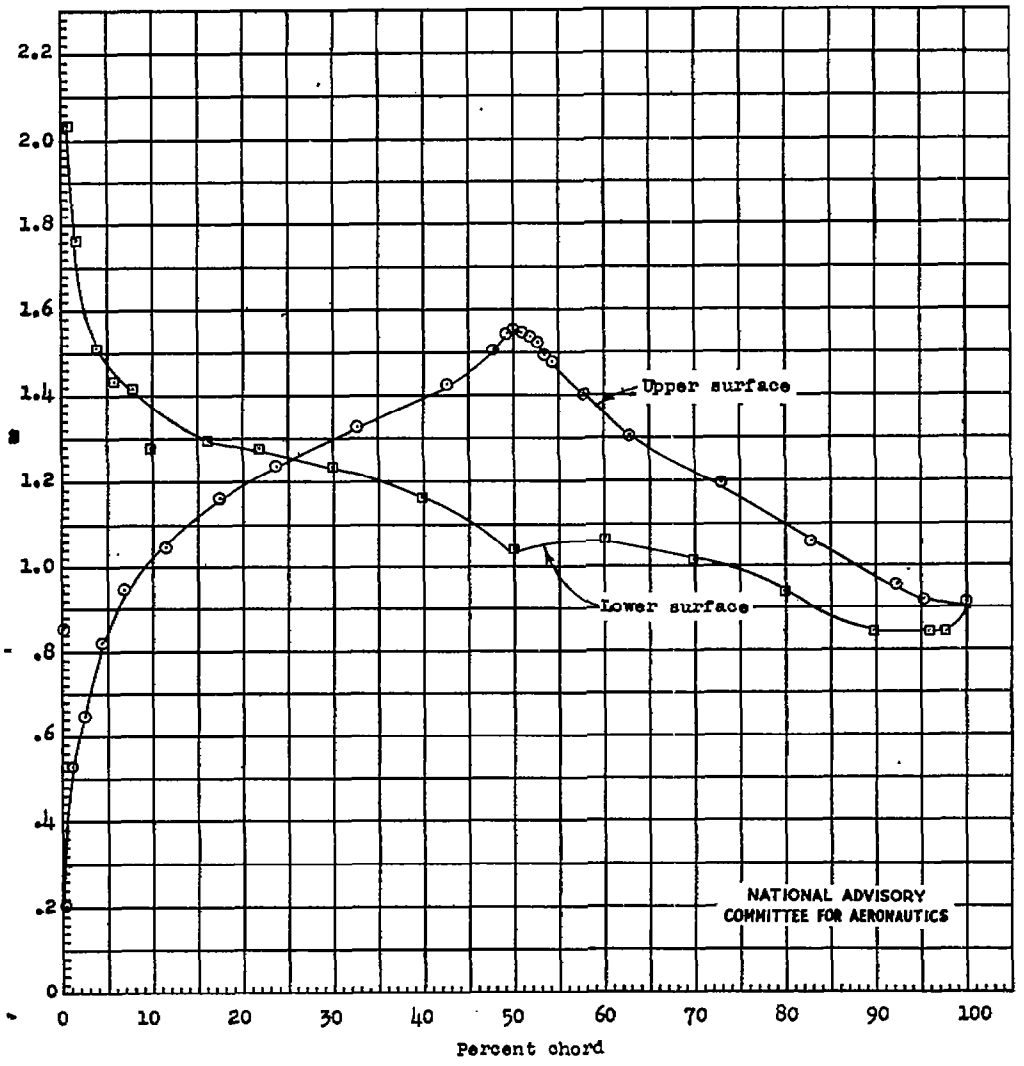

(e) $\alpha_o = -4.06^\circ$

Figure 6.- Continued.

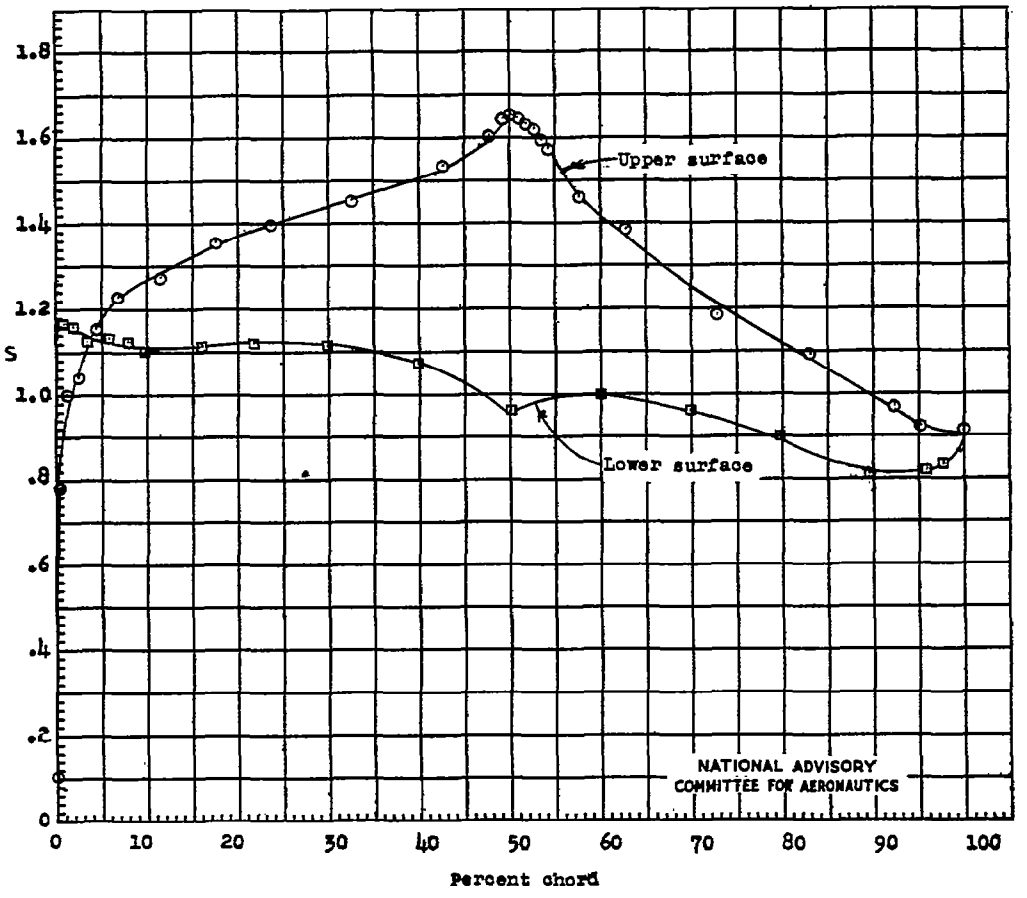

(f) $\alpha_o = -2.03^\circ$

Figure 6.- Continued.

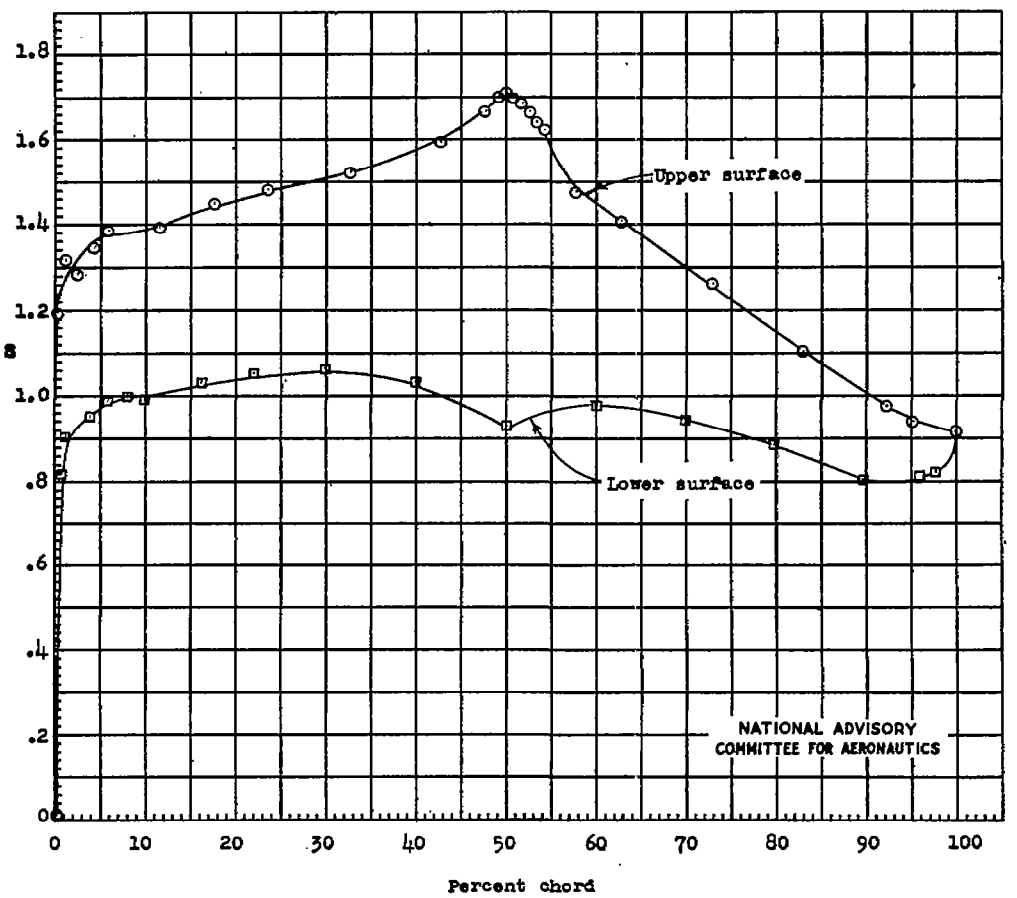

(g) $\alpha_o = -1.02^\circ$

Figure 6.- Continued.

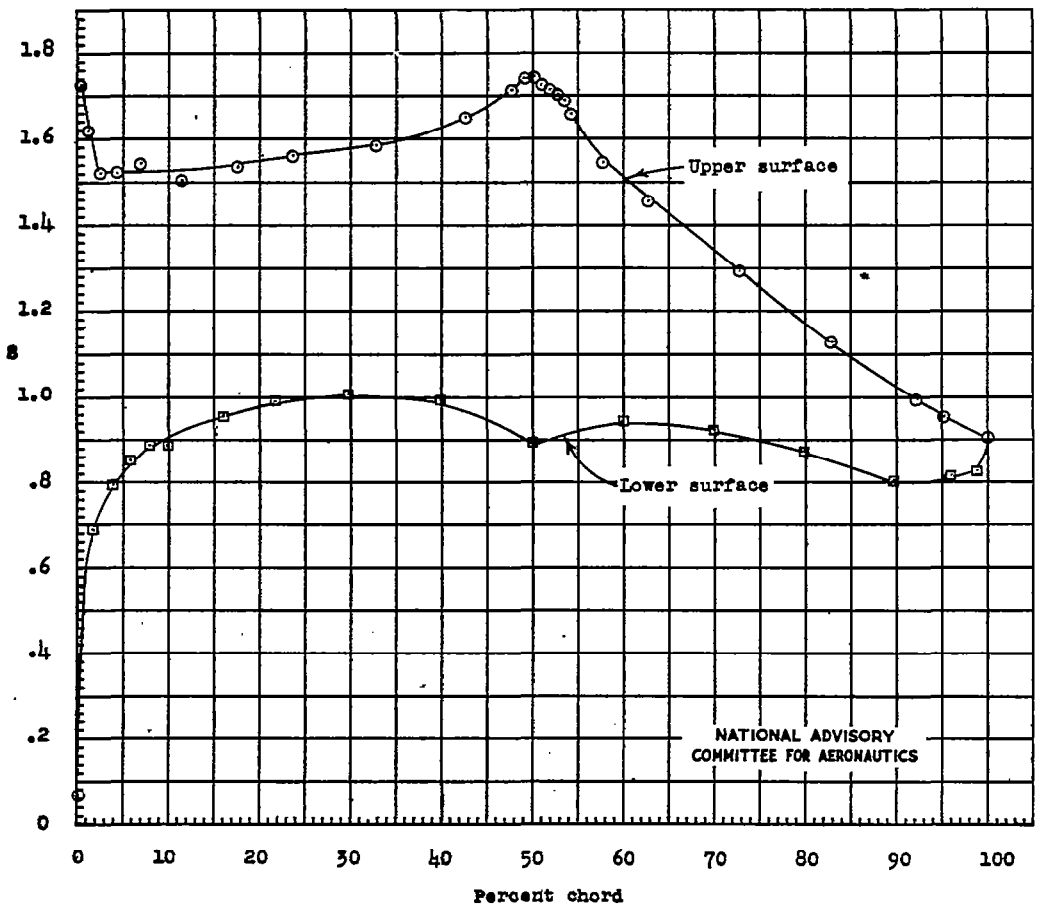

(h) $\alpha_o = 0^\circ$.

Figure 6.- Continued.

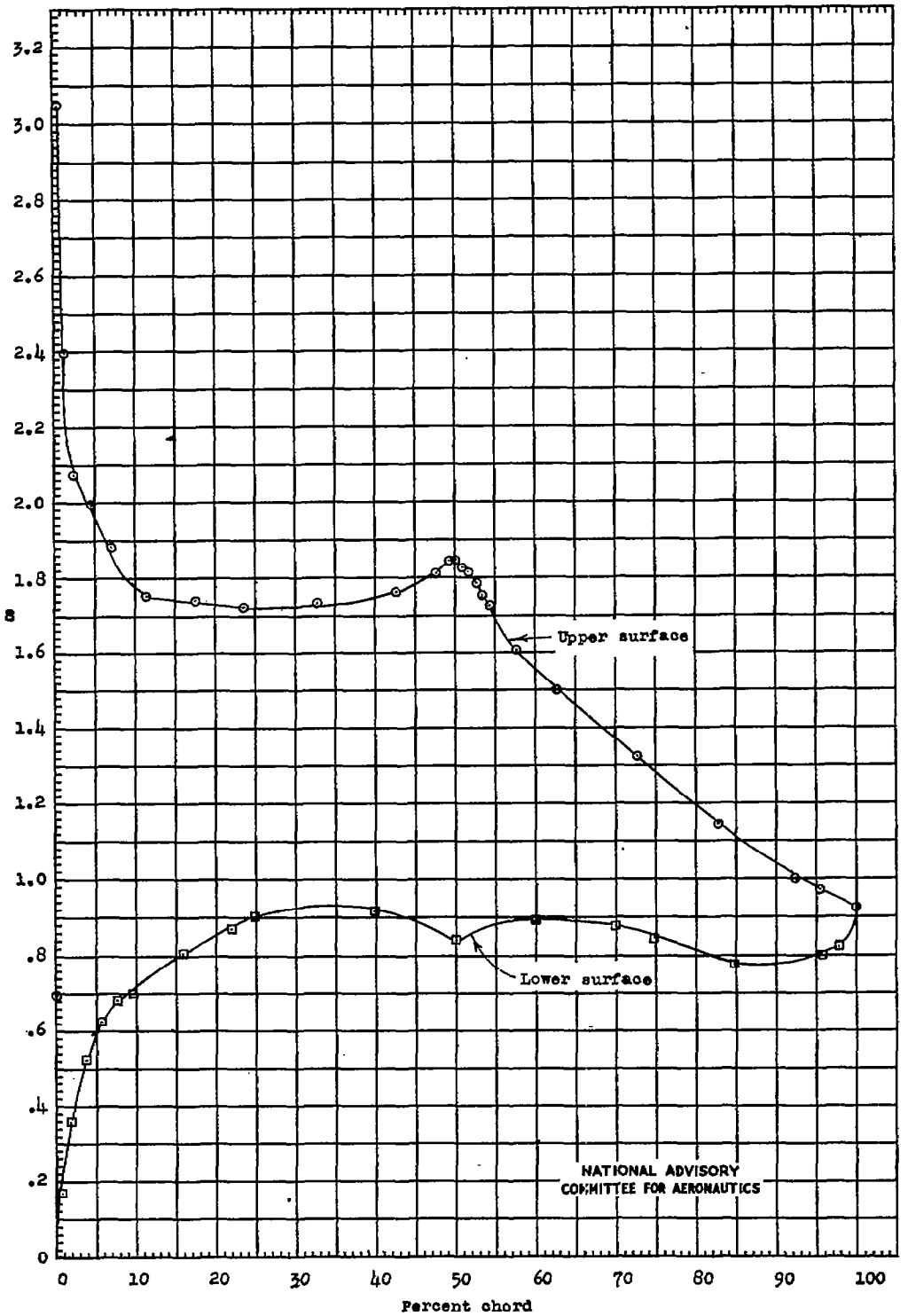

(i) $\alpha_0 = 2.03^\circ$.

Figure 6.- Continued.

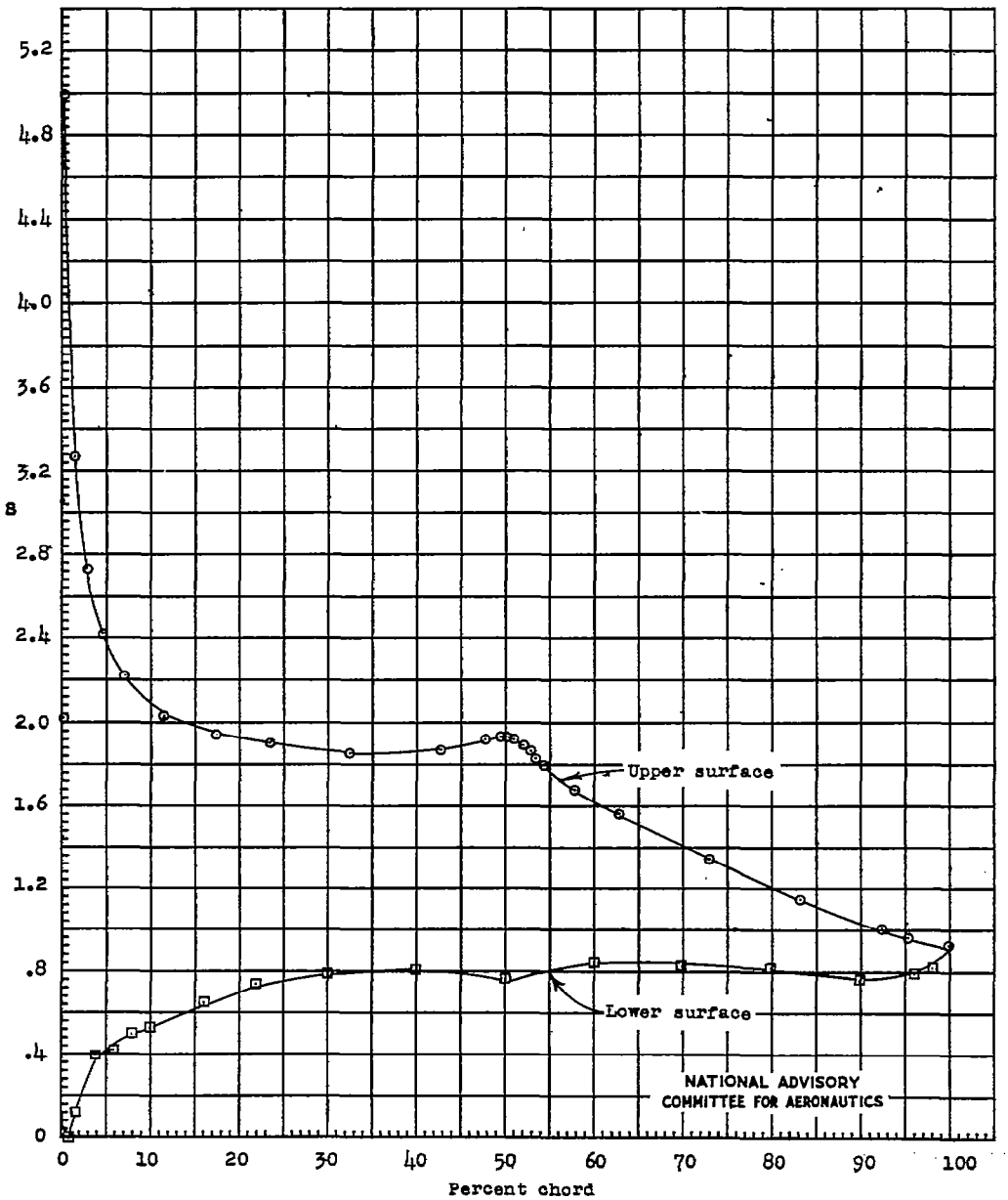

(j) $\alpha_o = 4.06^\circ$

Figure 6.- Continued.

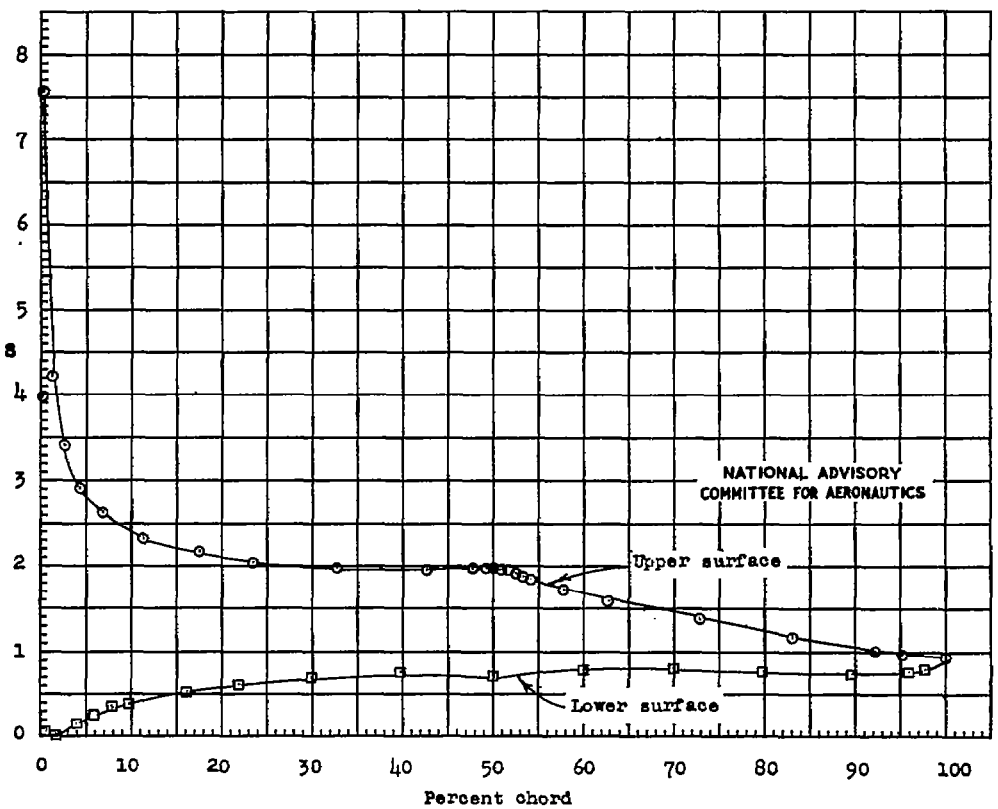

(k) $\alpha_0 = 6.09^\circ$.

Figure 6.- Continued.

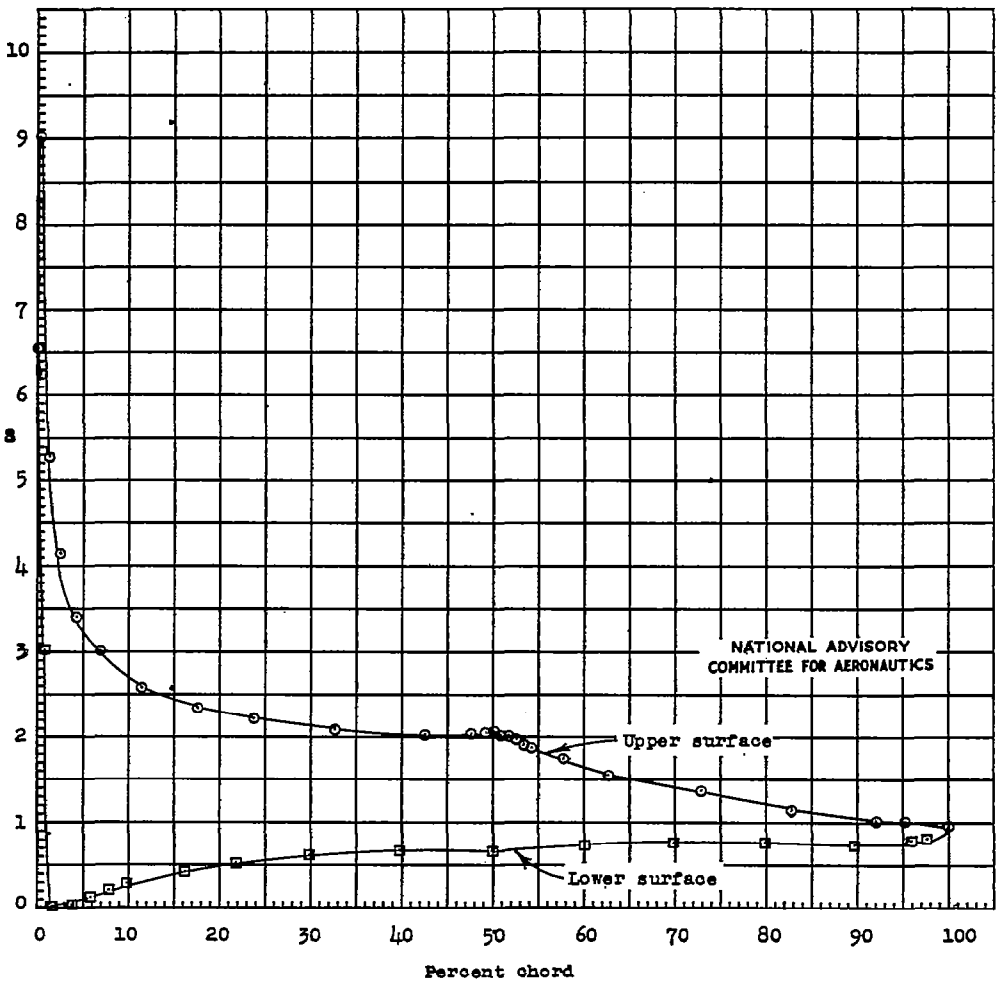

(1) $\alpha_o = 8.12^\circ$

Figure 6.- Continued.

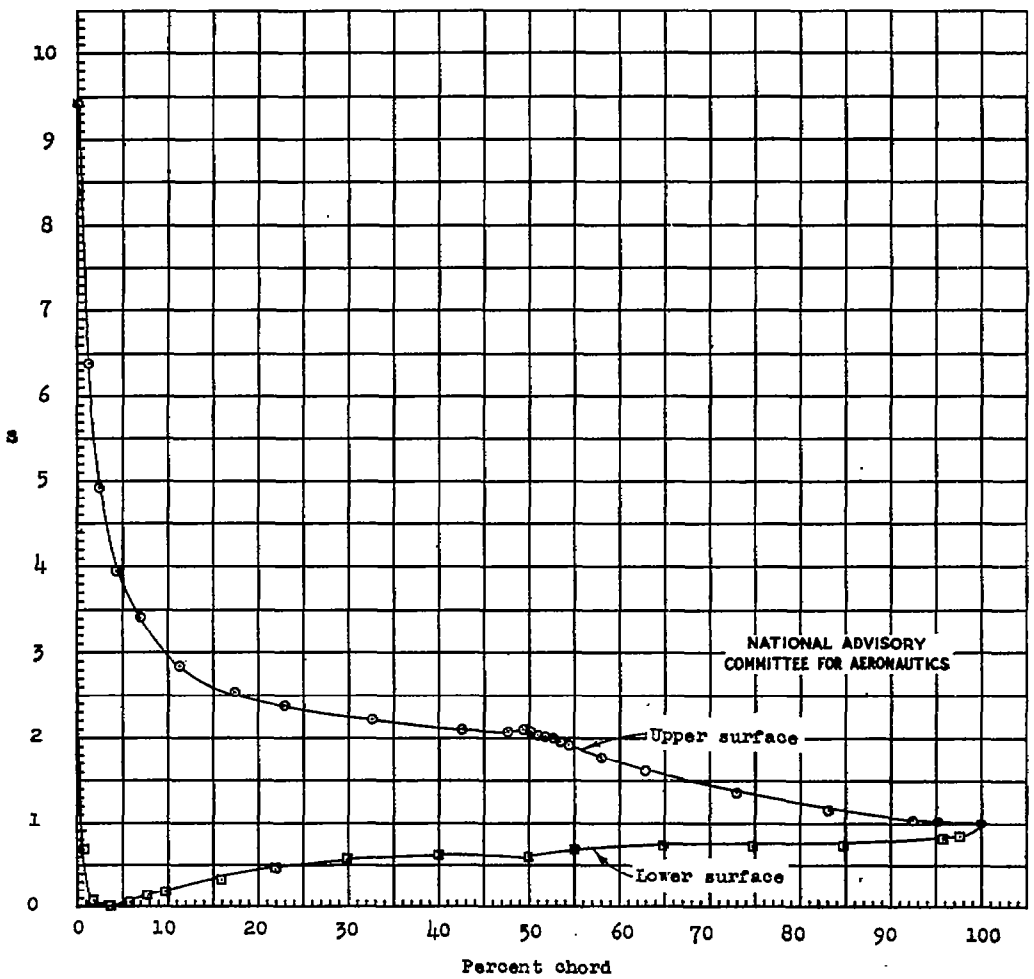

(m) $\alpha_o = 10.15^\circ$

Figure 6.- Continued.

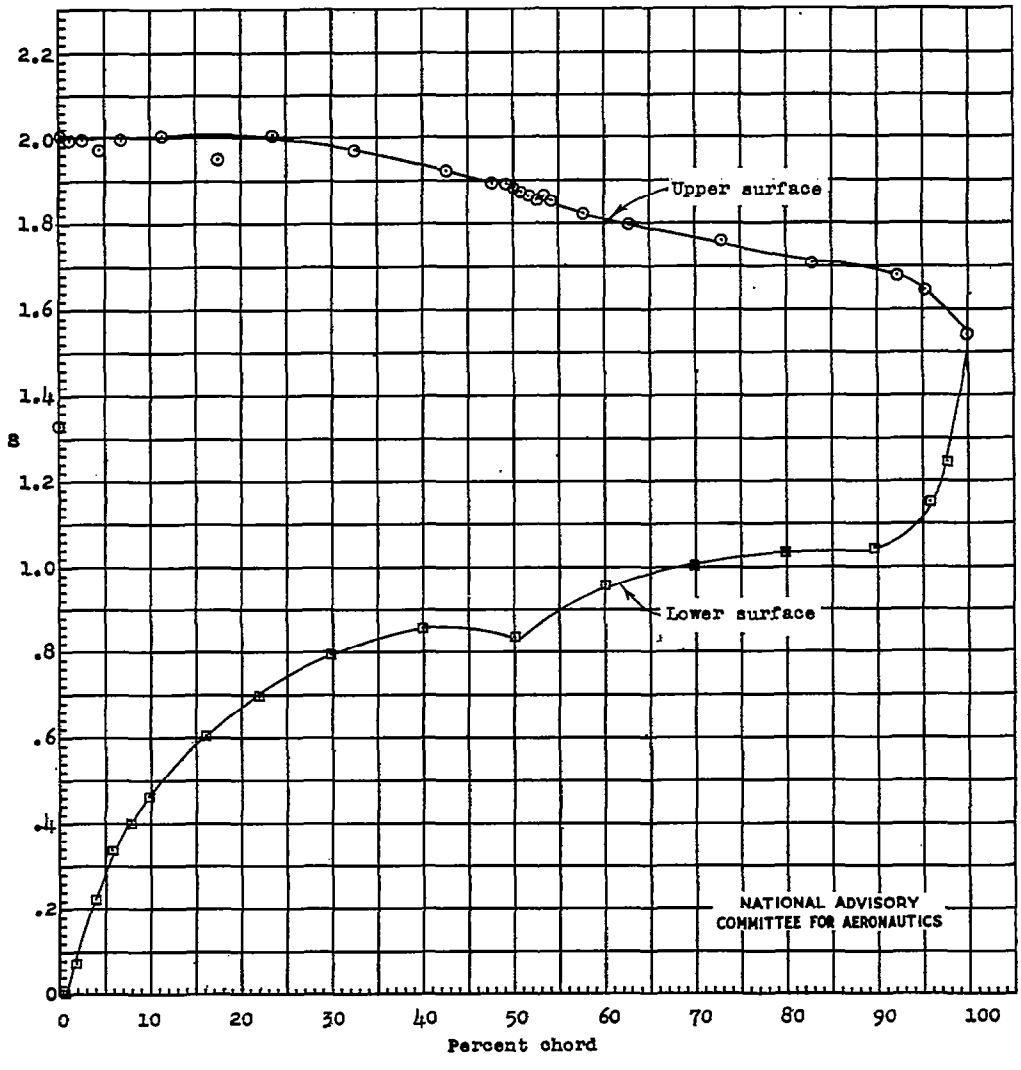

(n) $\alpha_o = 12.18^\circ$

Figure 6.- Concluded.

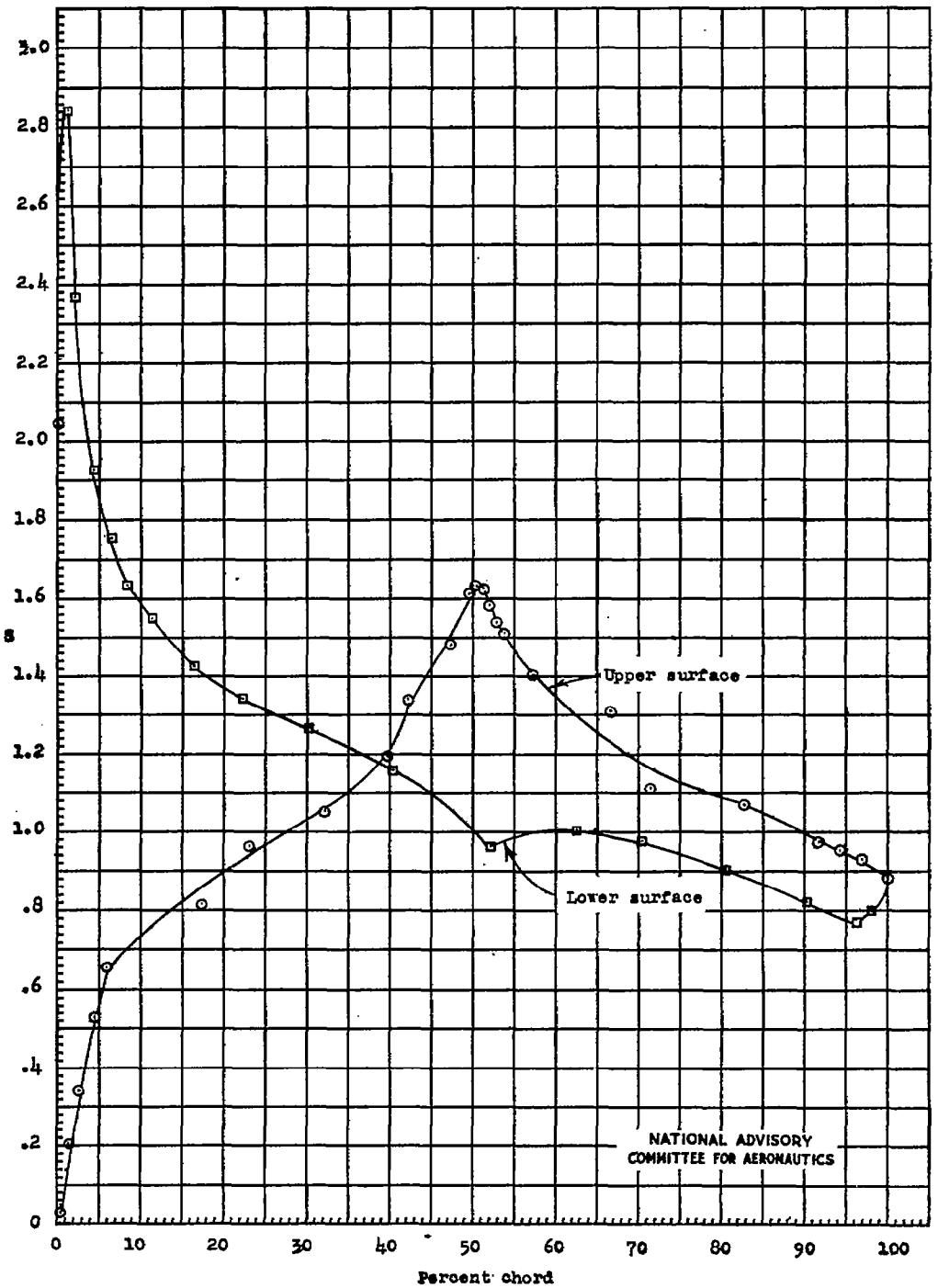

(a) $\alpha_o = -8.12^\circ$

Figure 7.- Pressure distribution for the NACA 65-210 airfoil section. $\delta_f = 7^\circ$; $R = 6.0 \times 10^6$; TDT test 874.

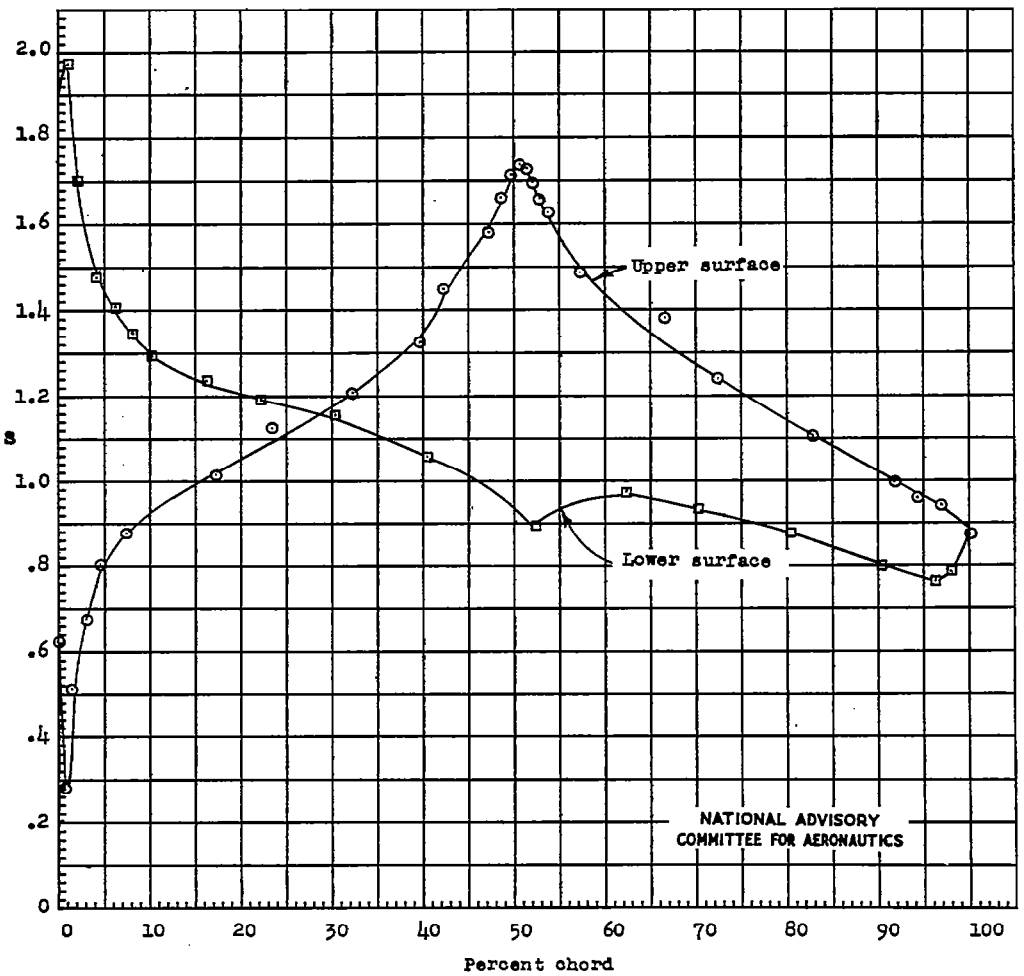

(b) $\alpha_o = -6.09^\circ$

Figure 7.- Continued.

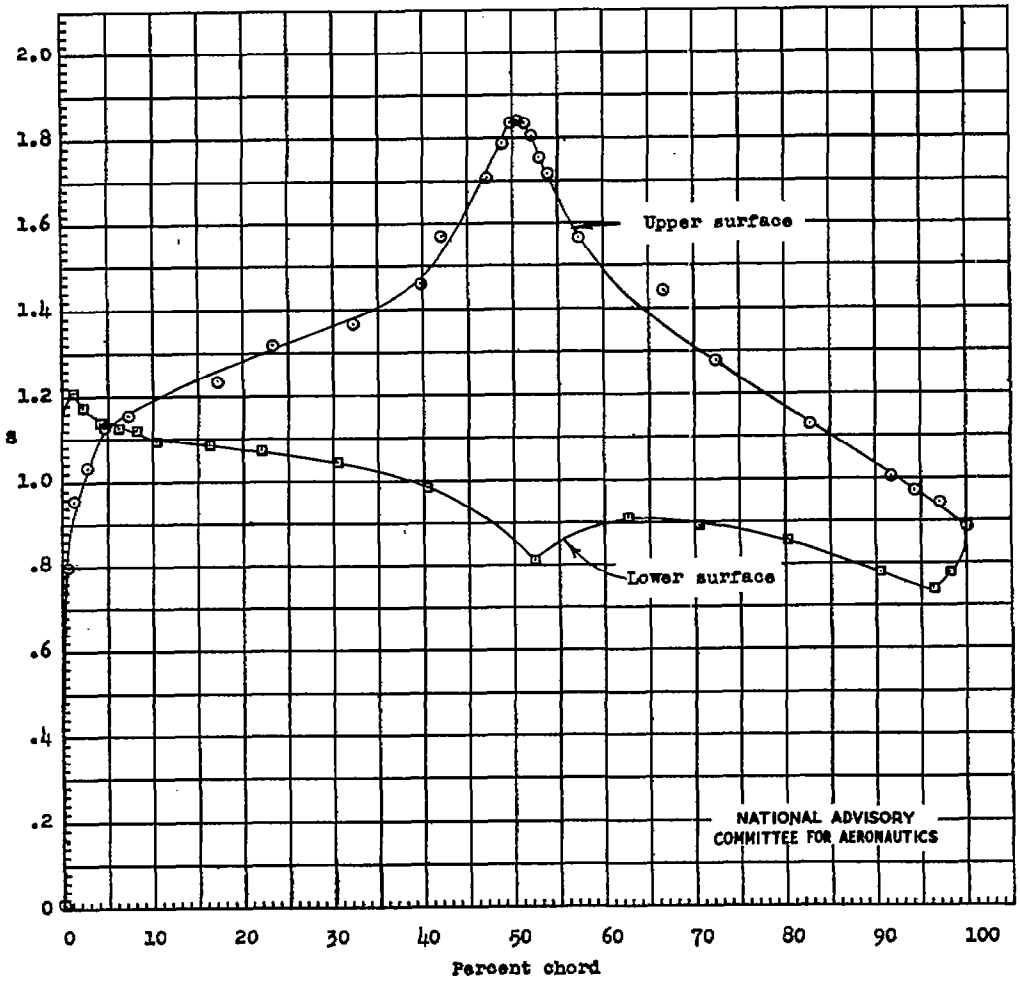

(c) $\alpha_o = -4.06°$

Figure 7.- Continued.

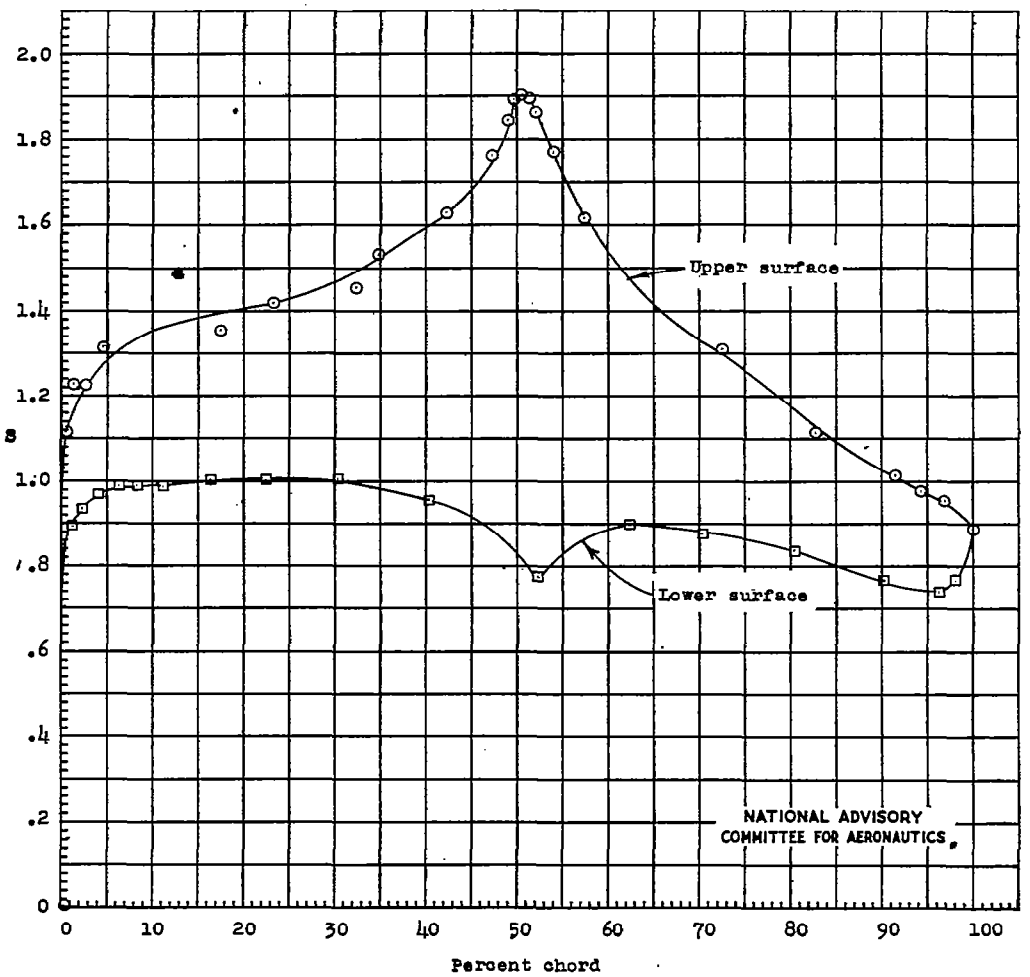

(d) $\alpha_o = -3.05^\circ$

Figure 7.- Continued.

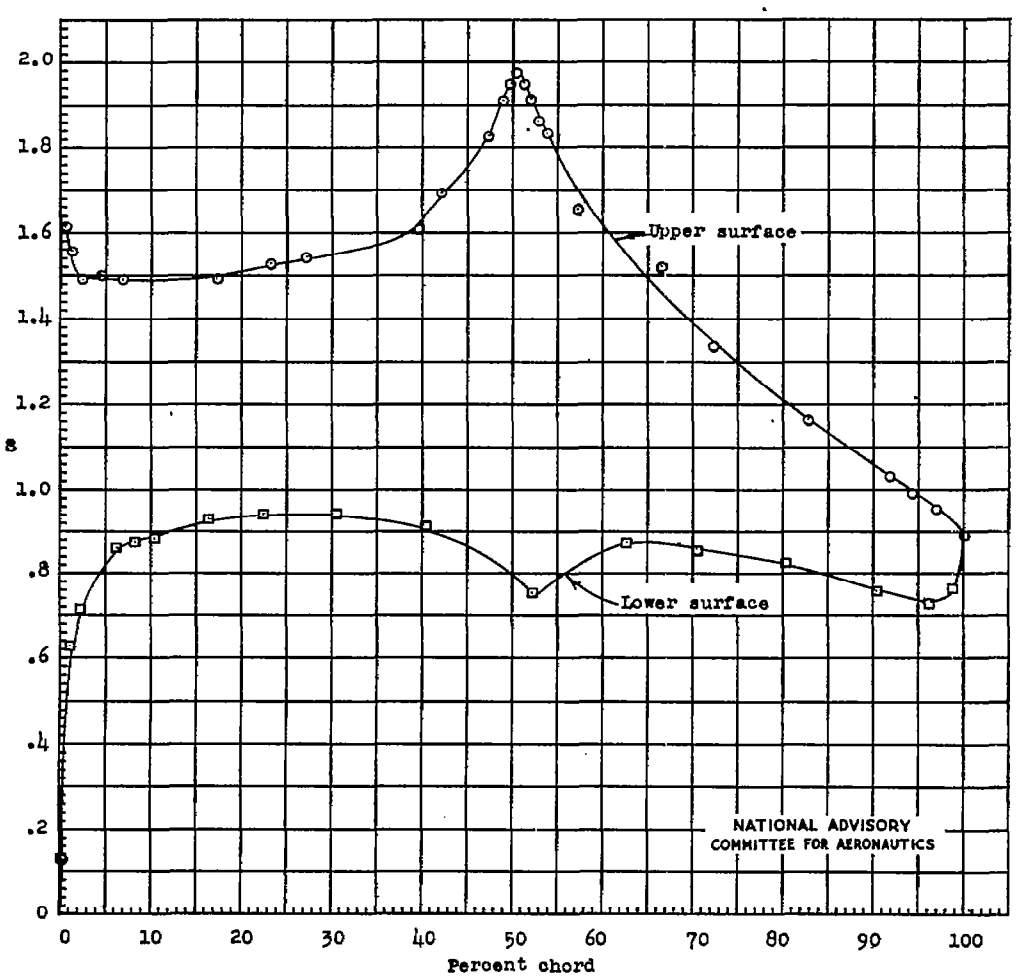

(e) $\alpha_o = -2.03^\circ$

Figure 7.- Continued.

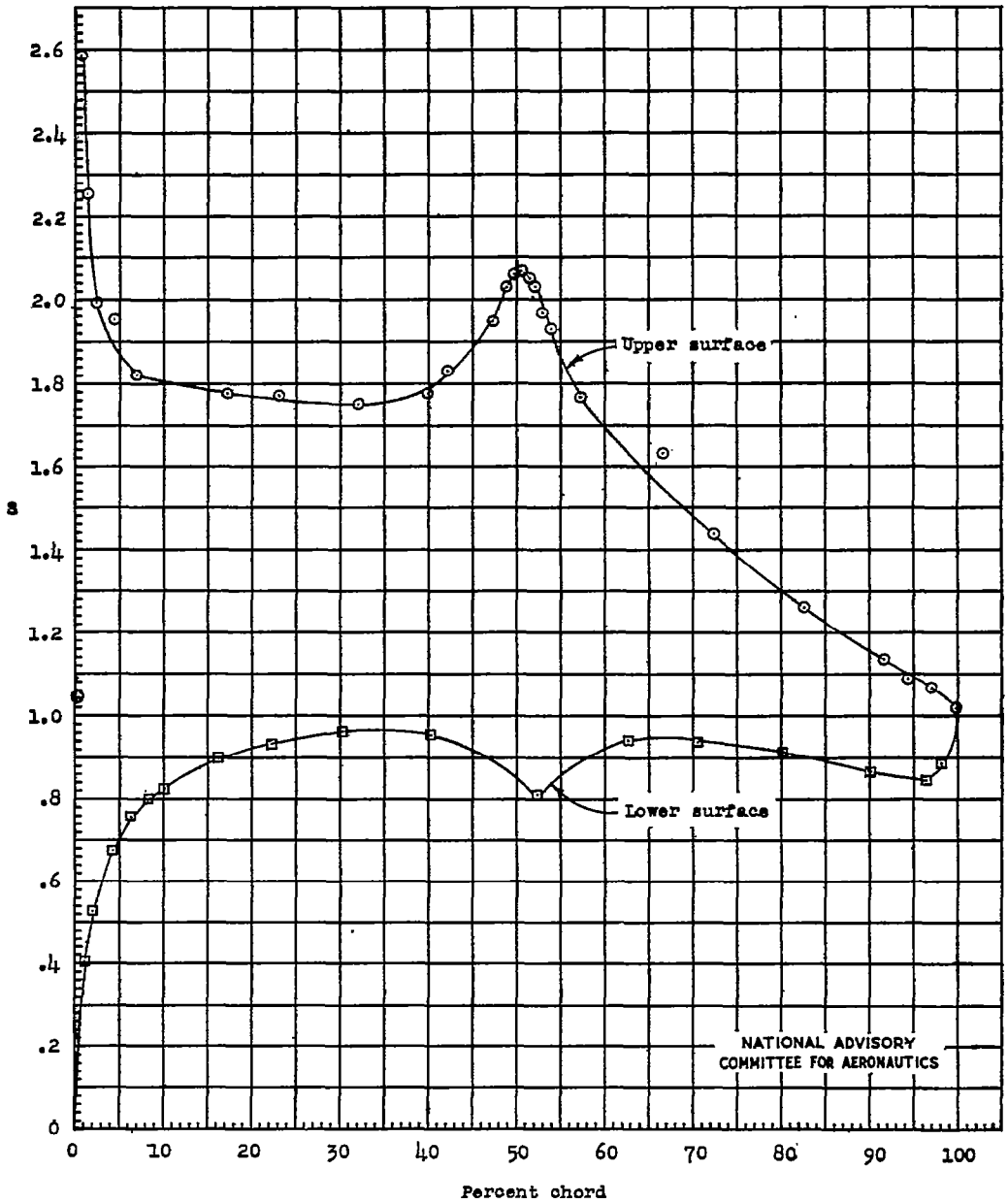

(f) $\alpha_o = 0^\circ$

Figure 7.- Continued.

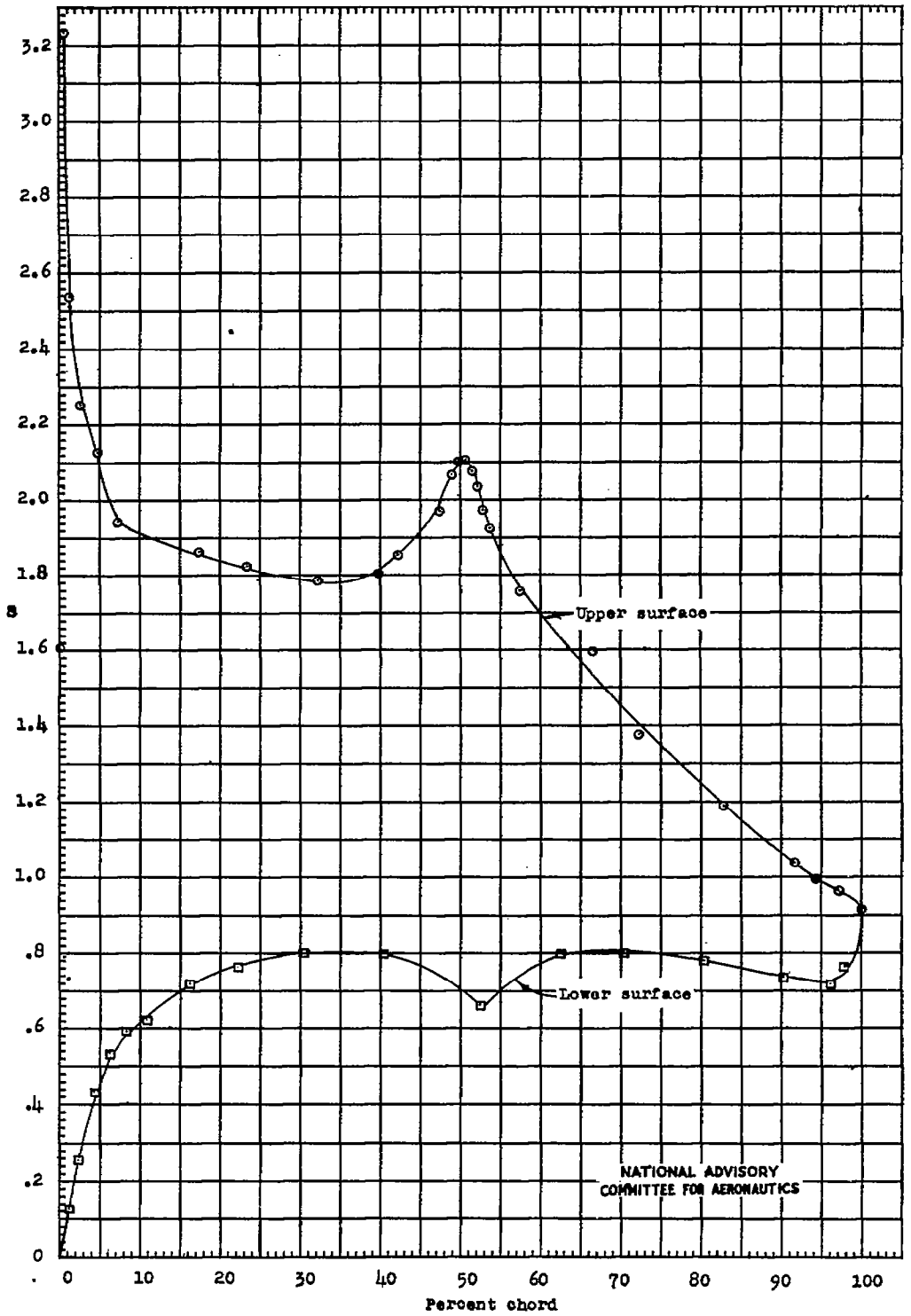

(g) $\alpha_o = 1.02^\circ$

Figure 7.- Continued.

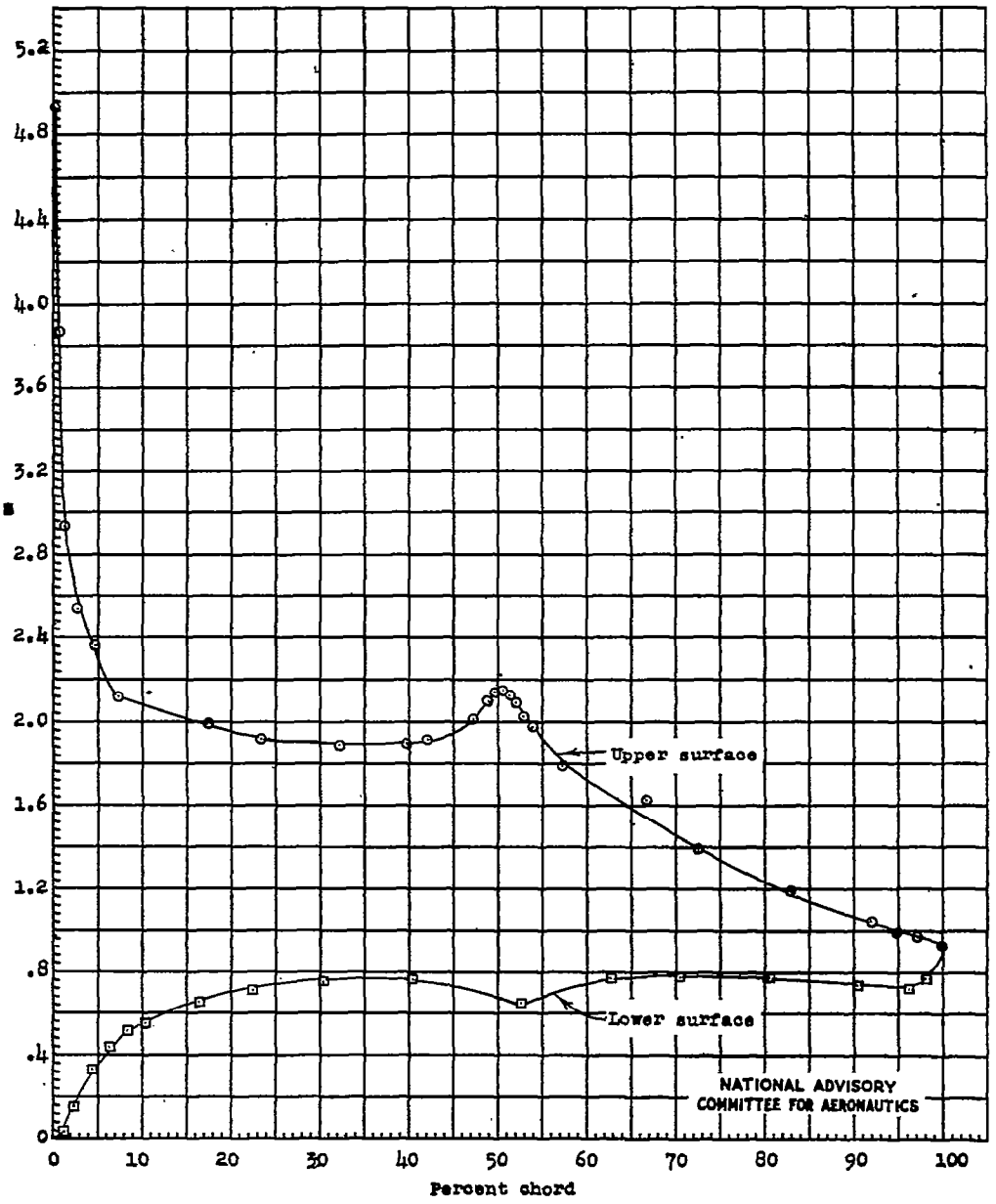

(h) $\alpha_o = 2.03^\circ$.

Figure 7.- Continued.

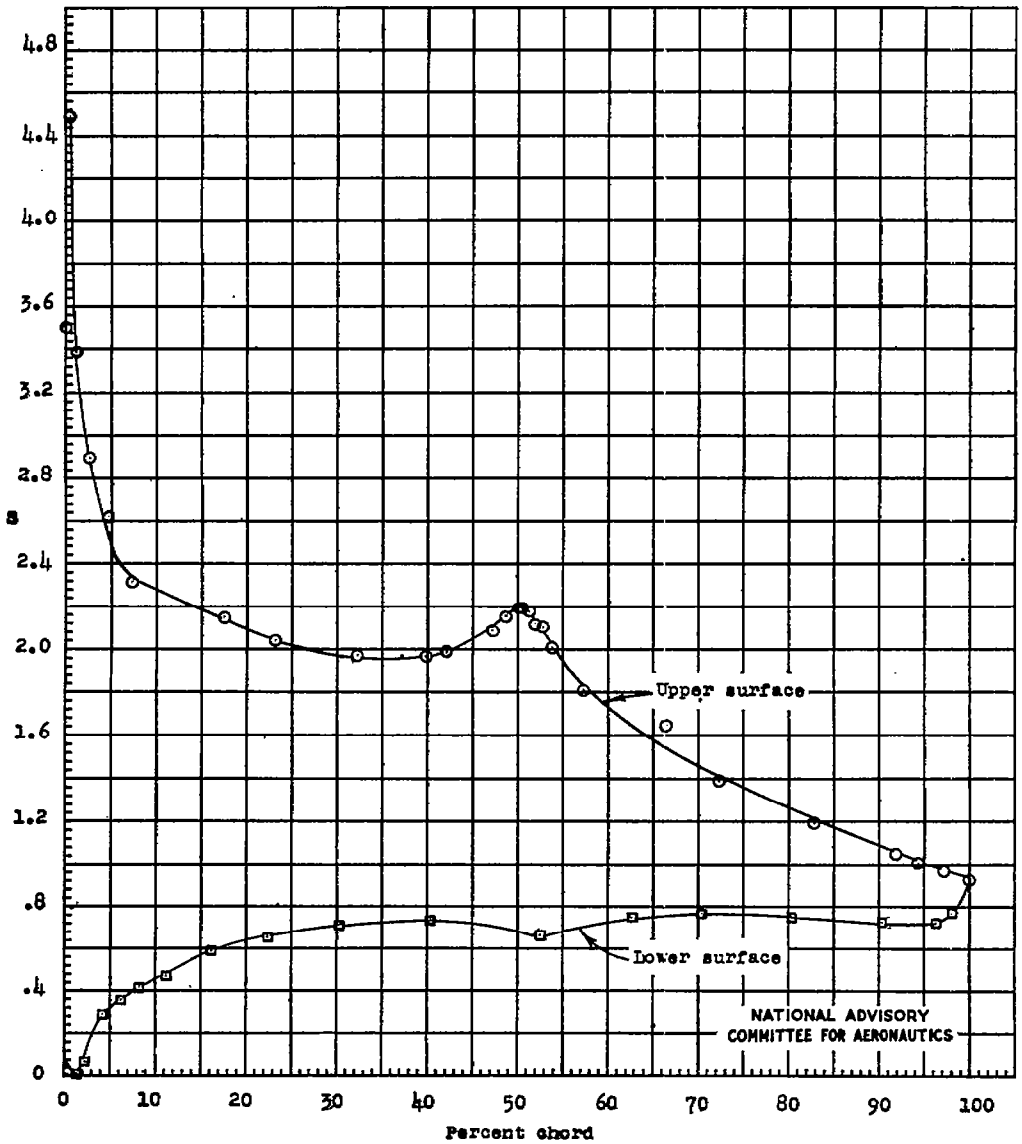

(i) $\alpha_o = 3.05^\circ$

Figure 7.- Continued.

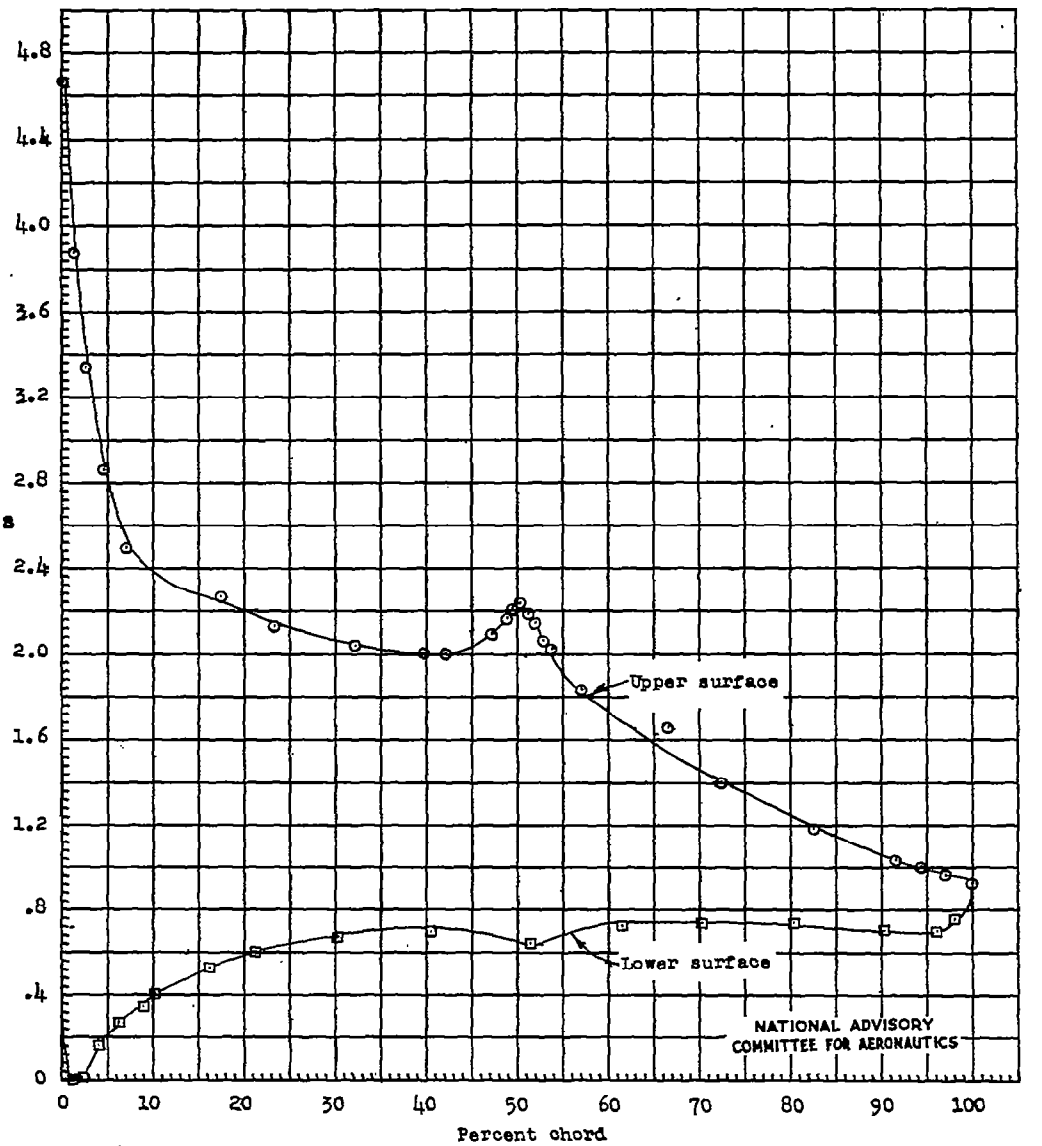

(j) $\alpha_o = 4.06^\circ$

Figure 7.- Continued.

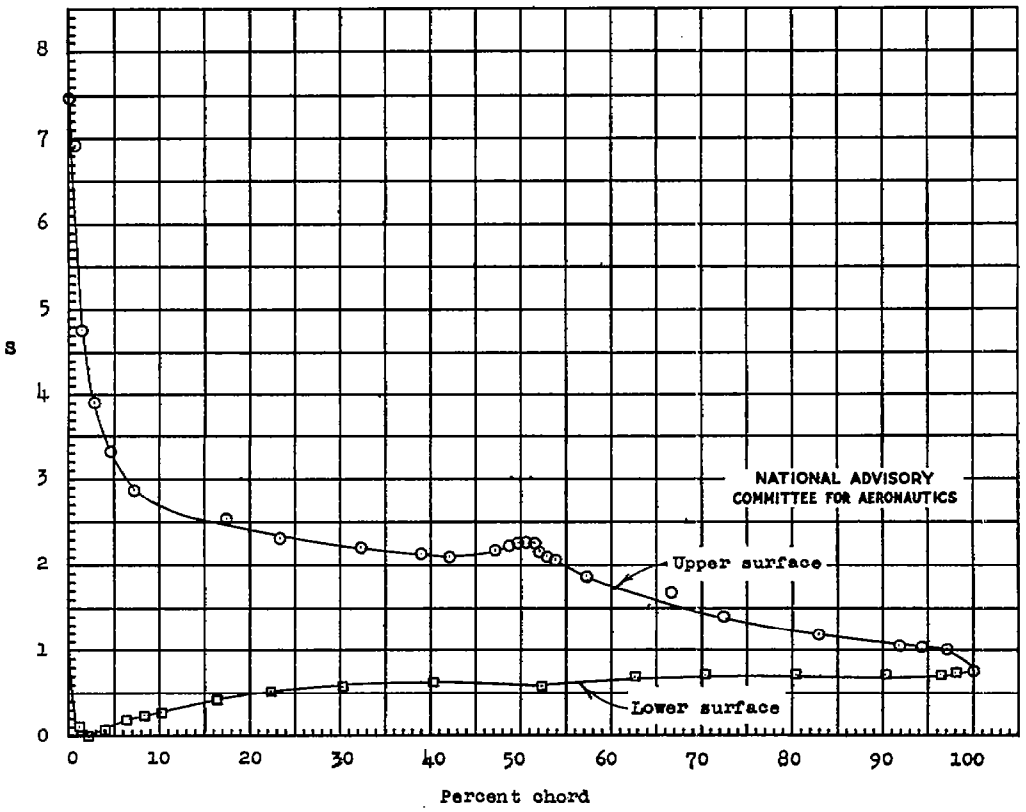

(k) $\alpha_0 = 6.09^\circ$

Figure 7.- Continued.

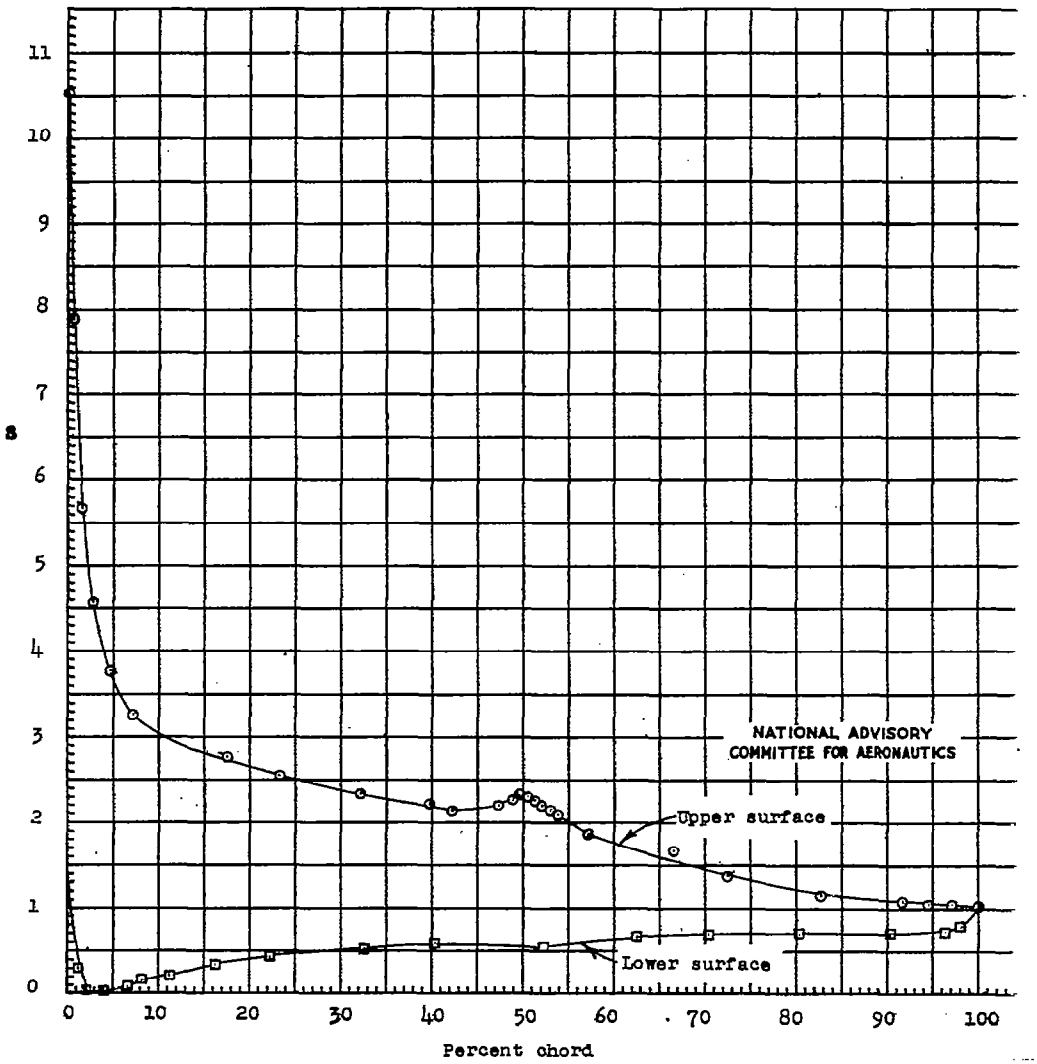

(1) $\alpha_o = 8.12^\circ$

Figure 7.- Continued.

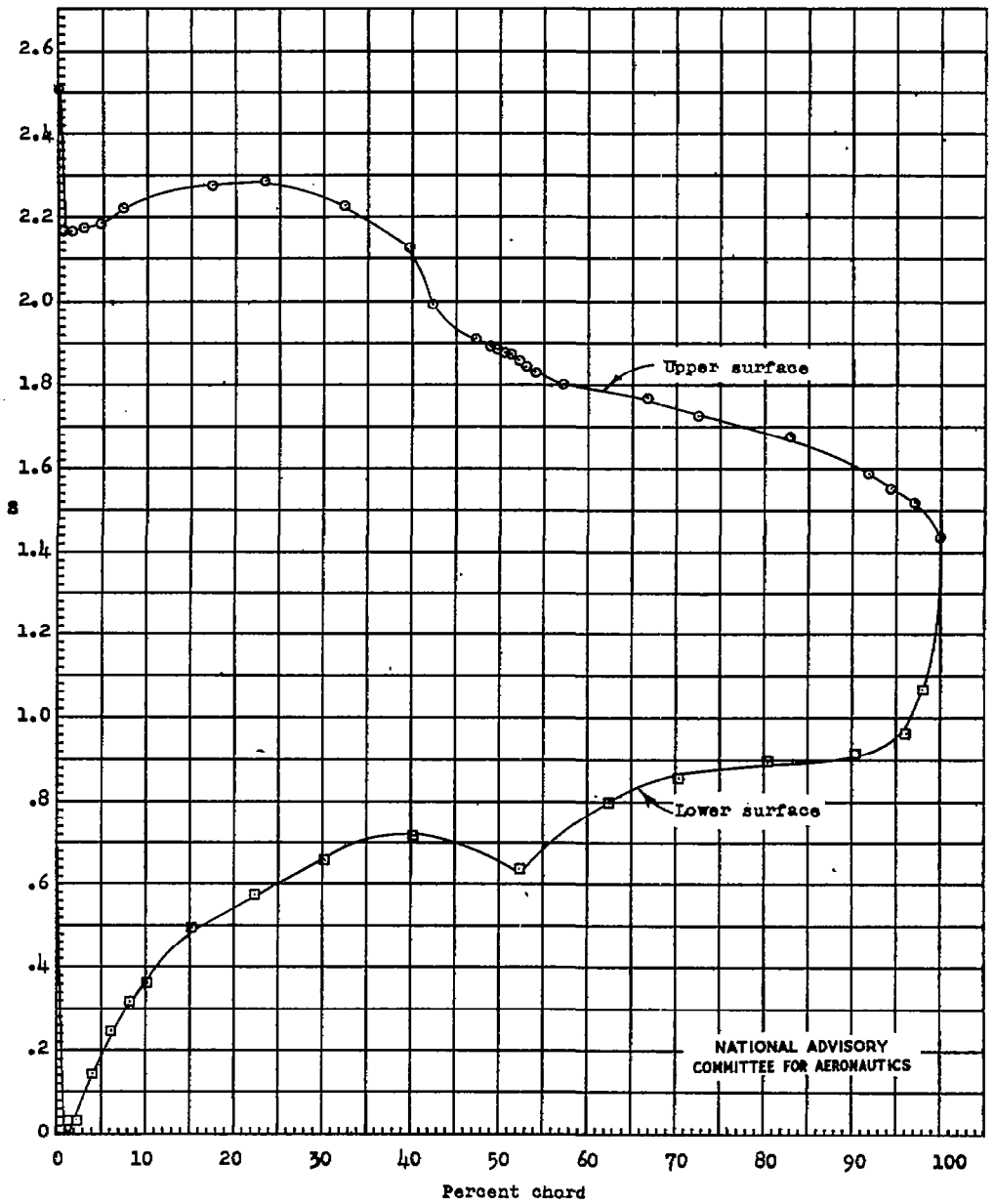

(m) $\alpha_o = 10.15^\circ$

Figure 7.- Continued.

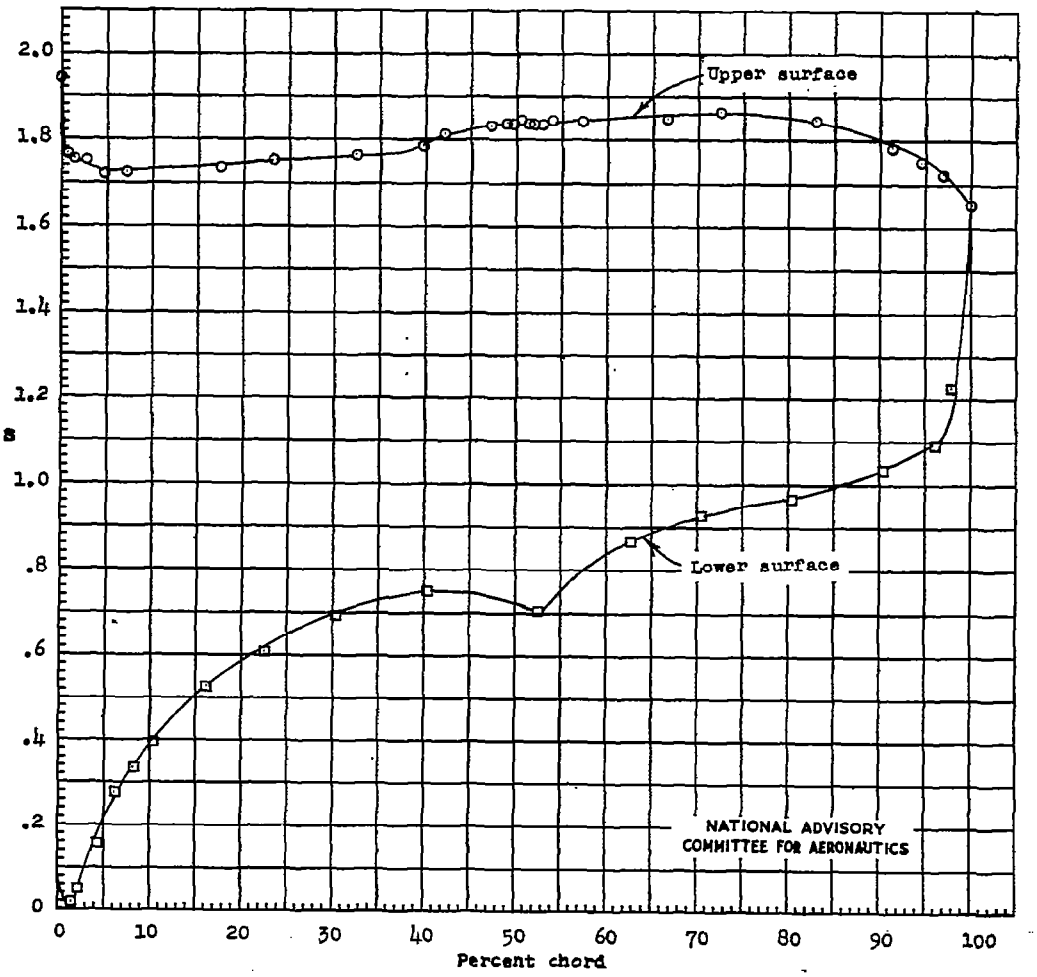

(n) $\alpha_o = 12.15^\circ$.

Figure 7.- Concluded.

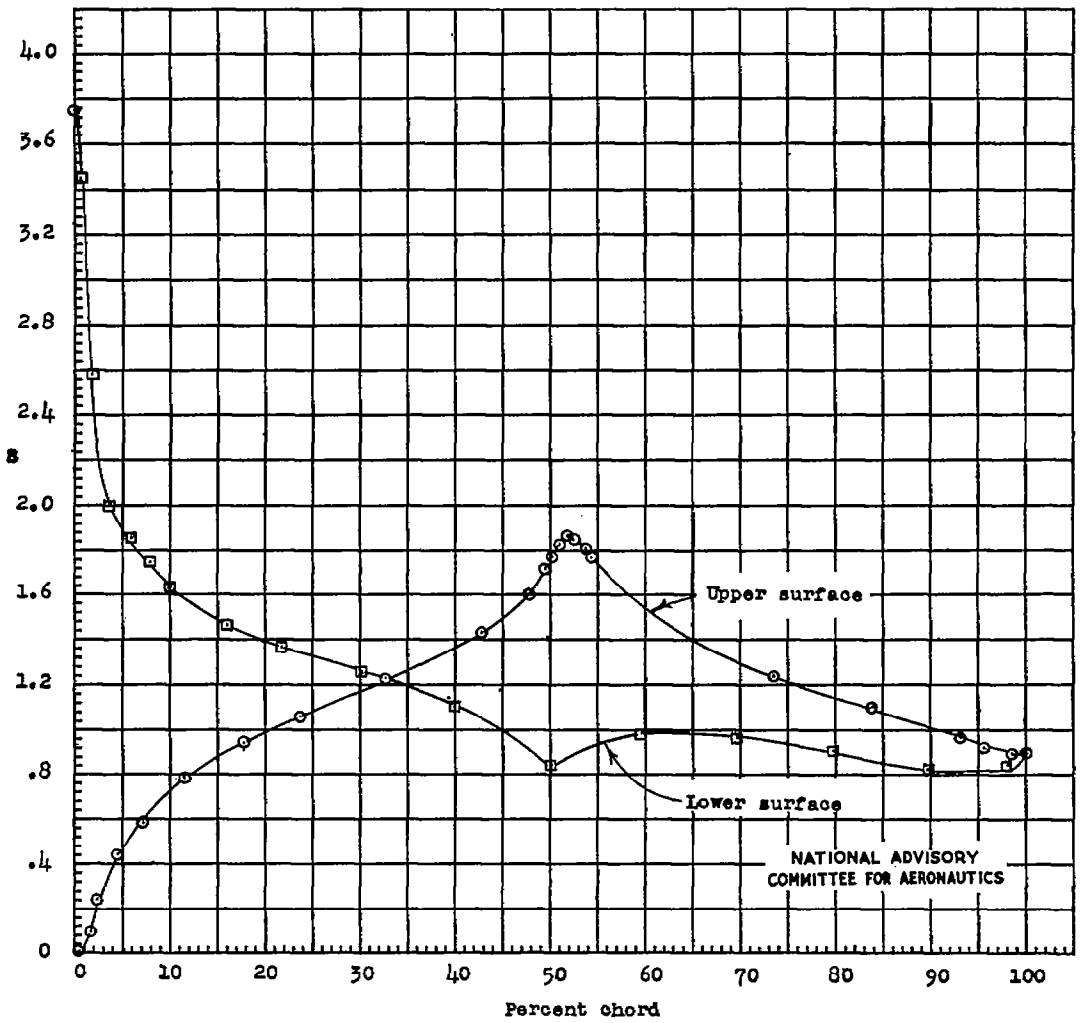

(a) $\alpha_o = -10.15^\circ$.

Figure 8.- Pressure distribution for the NACA 65-210 airfoil. $\delta_f = 10^\circ$; $R = 6.0 \times 10^6$; TDT test 874.

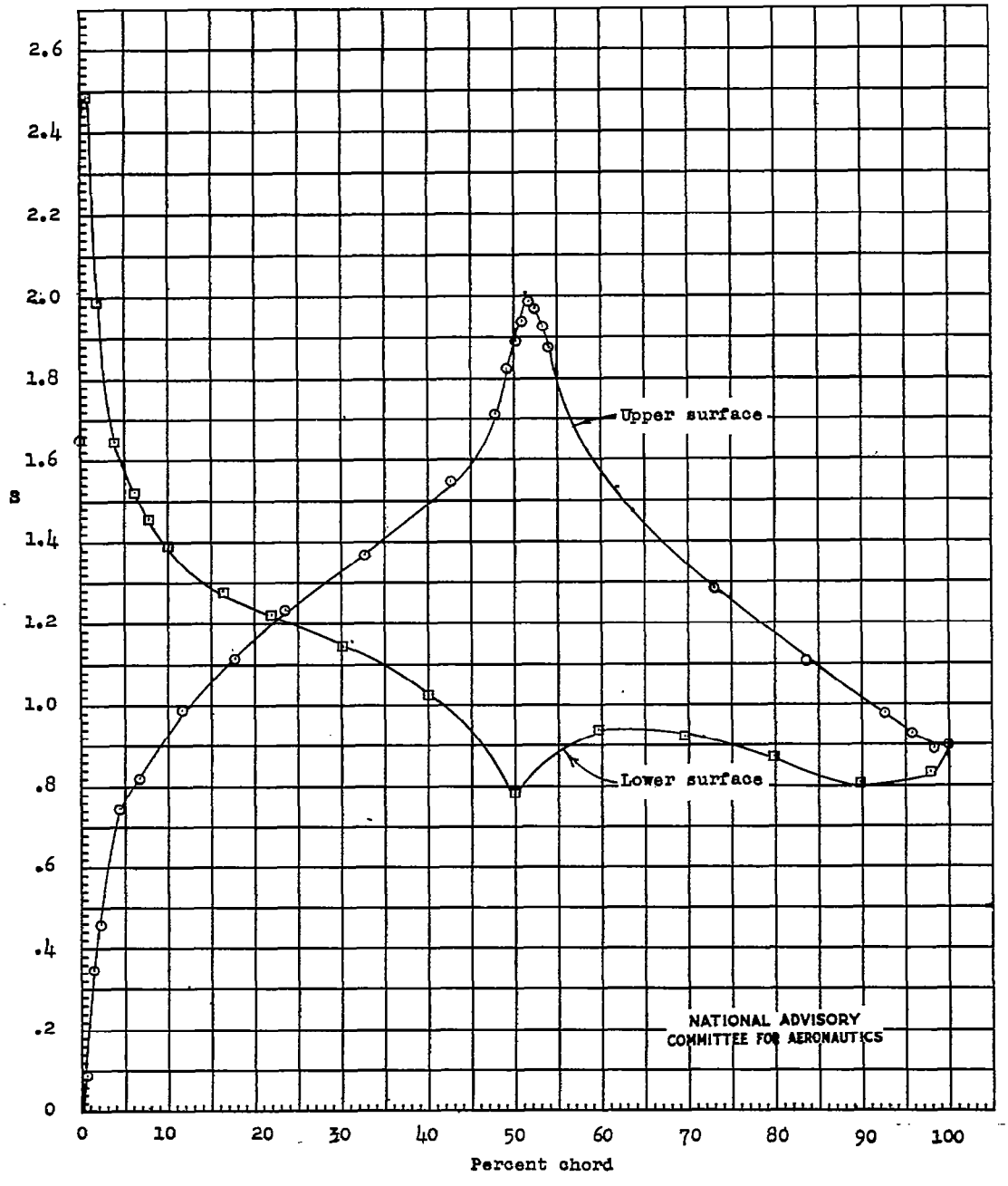

(b) $\alpha_o = -8.12^\circ$

Figure 8.- Continued.

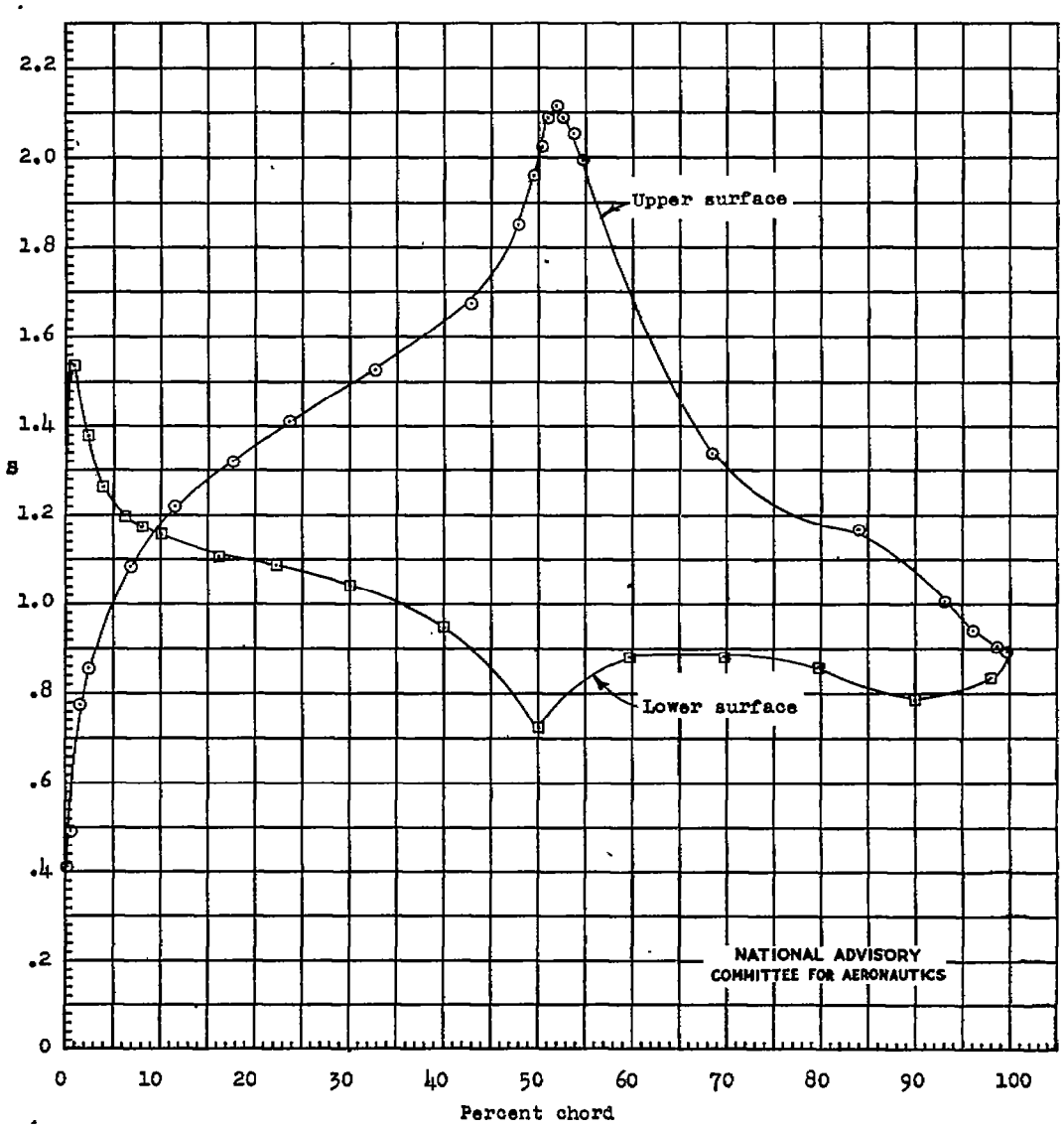

(c) $\alpha_o = -6.09^\circ$

Figure 8.- Continued.

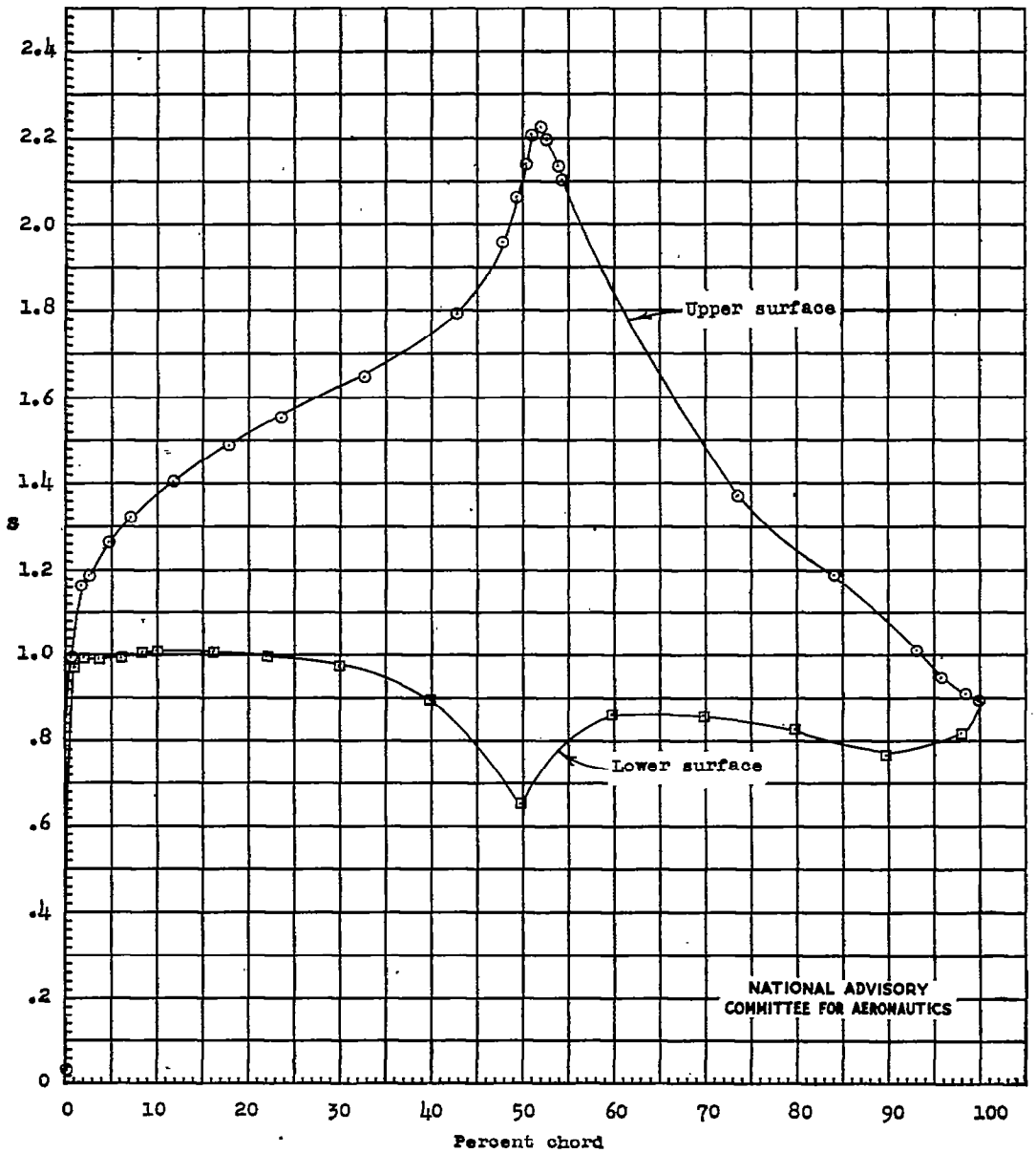

(d) $\alpha_o = -4.57^\circ$

Figure 8.- Continued.

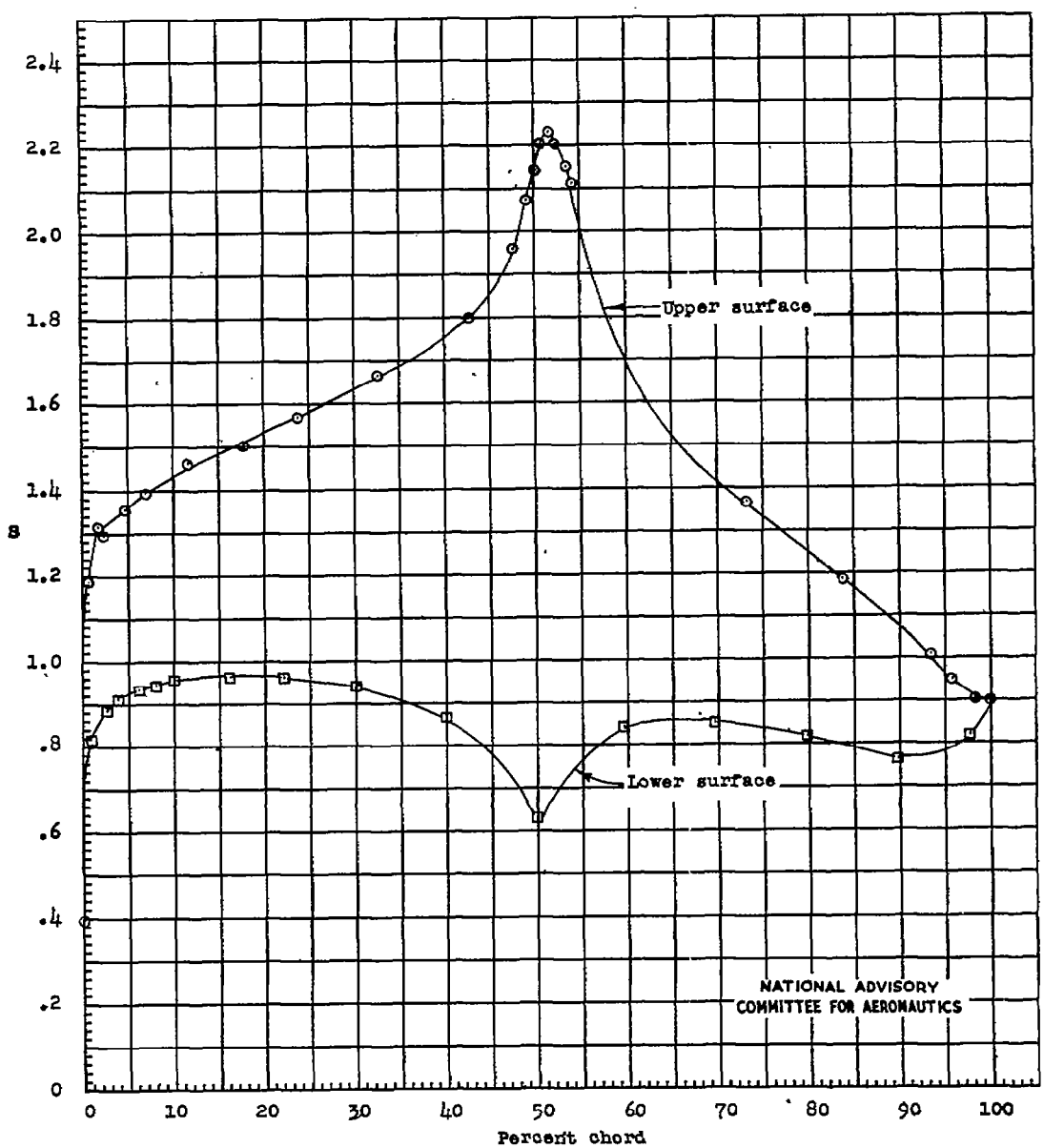

(e) $\alpha_o = -4.06^\circ$.

Figure 8.- Continued.

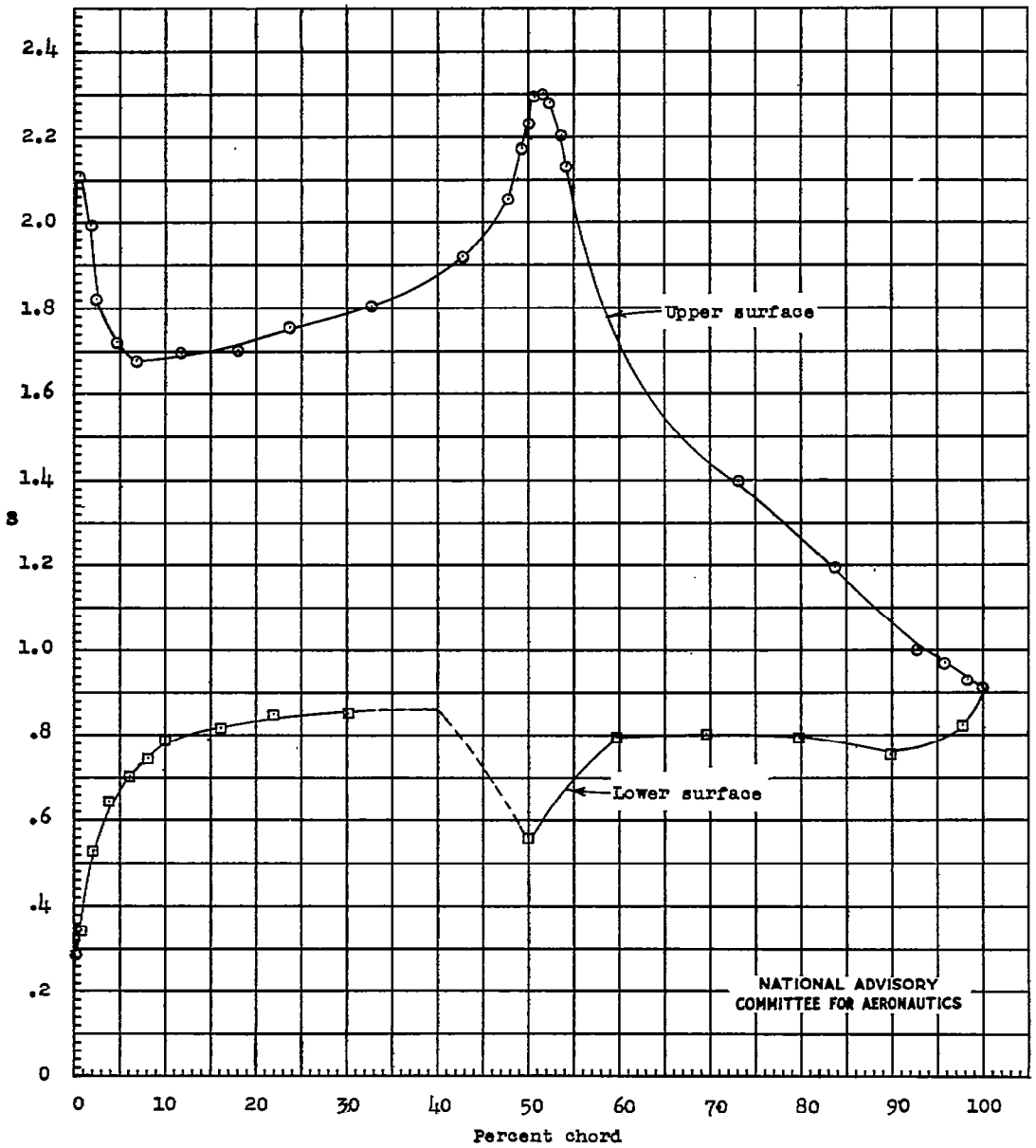

(f) $\alpha_o = -2.03^\circ$

Figure 8.- Continued.

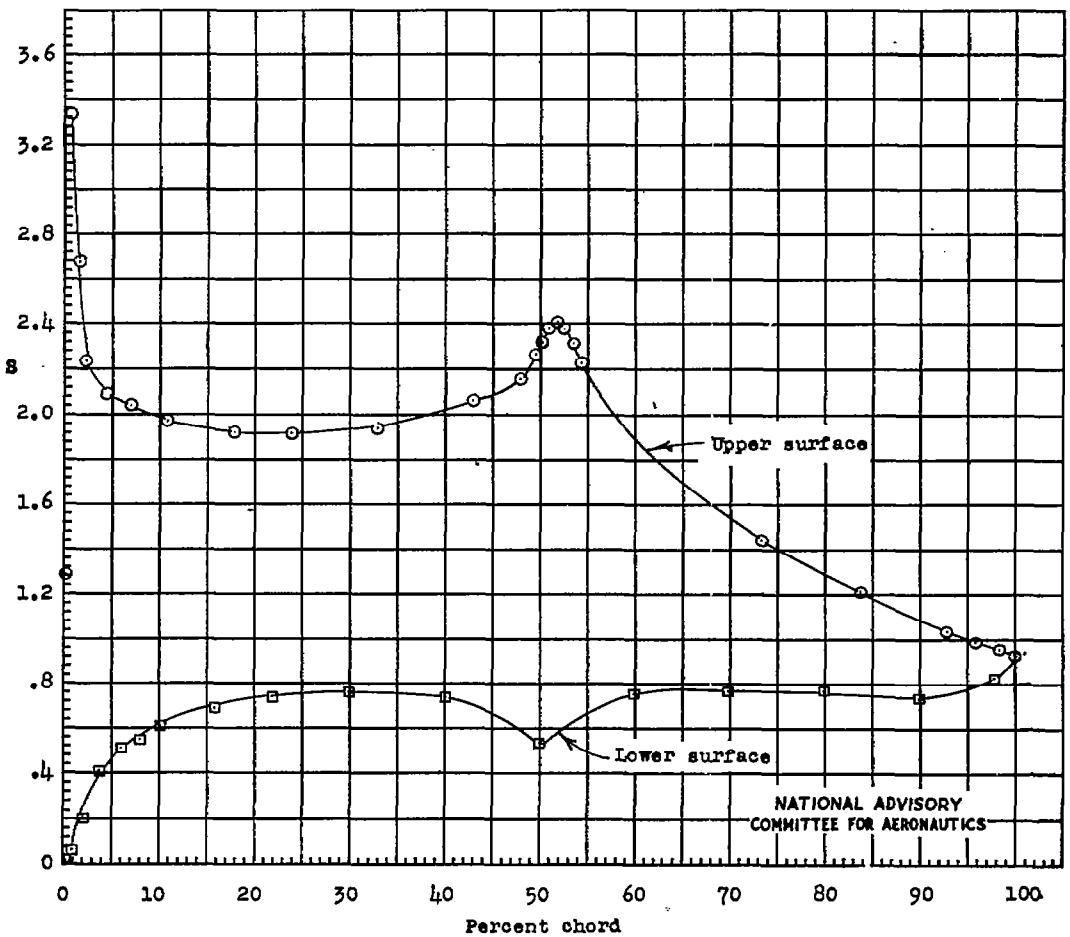

(g) $\alpha_o = 0^\circ$

Figure 8.- Continued.

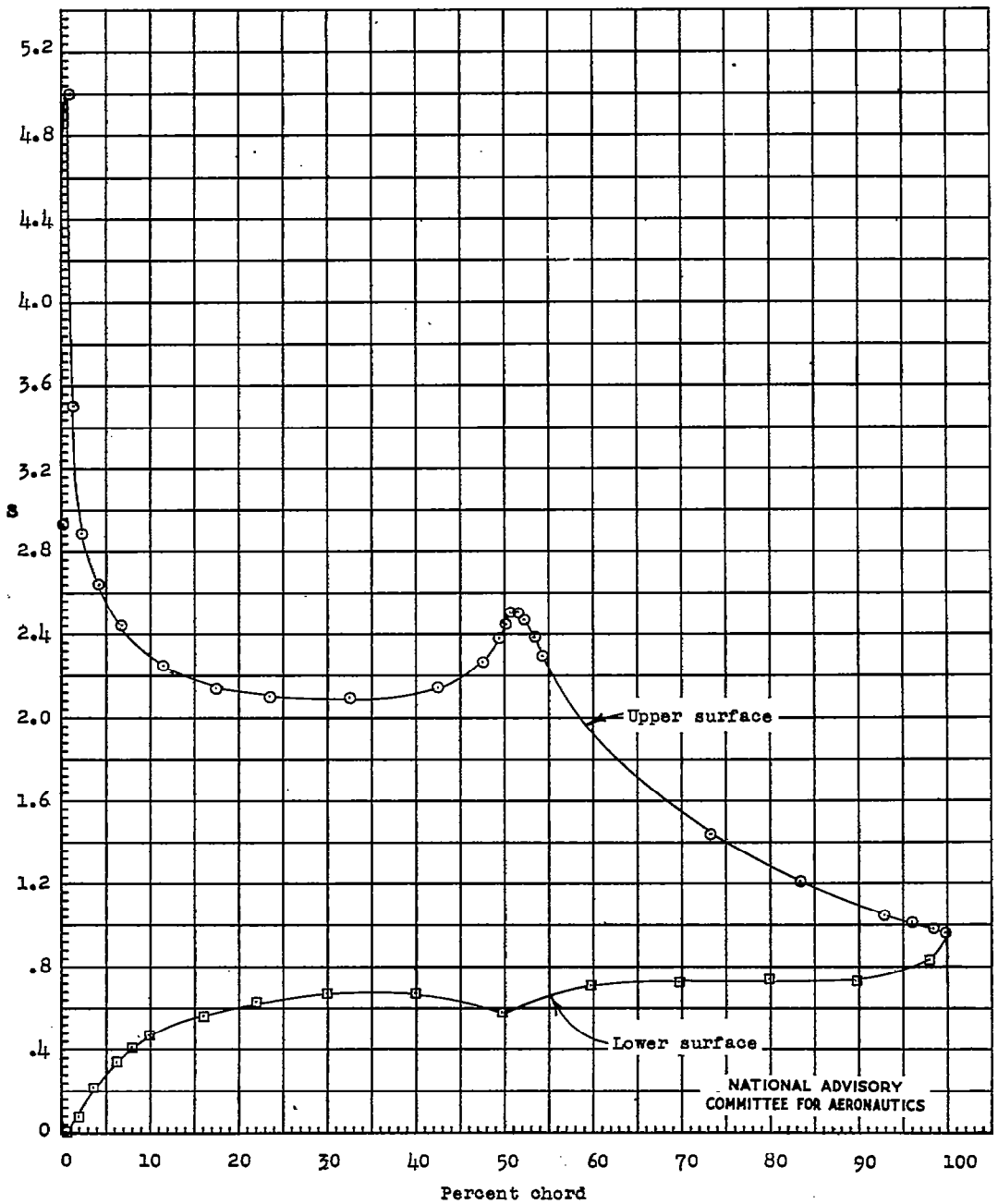

(h) $\alpha_o = 2.03^\circ$.

Figure 8.- Continued.

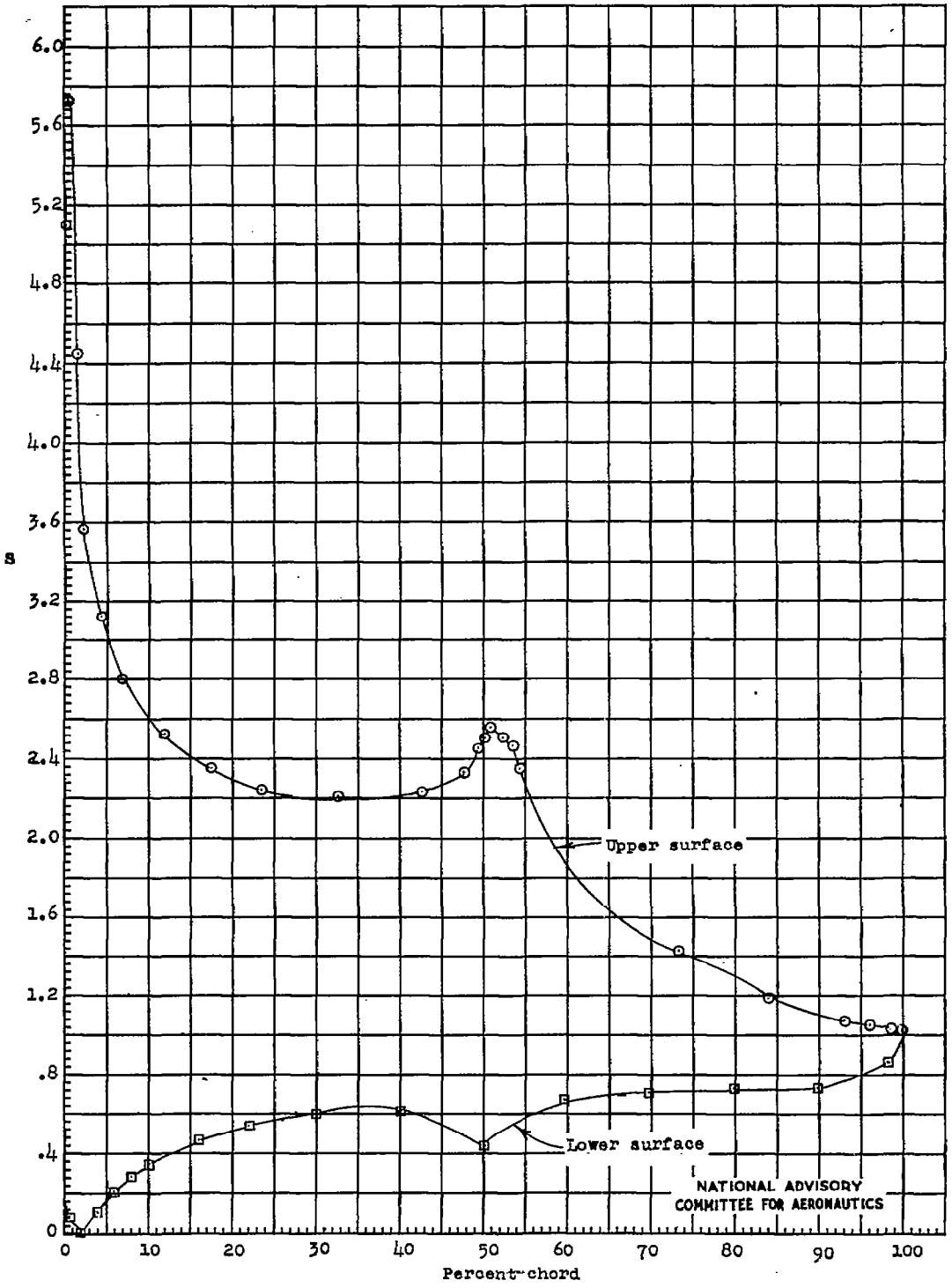

(i) $\alpha_o = 4.06^\circ$

Figure 8.- Continued.

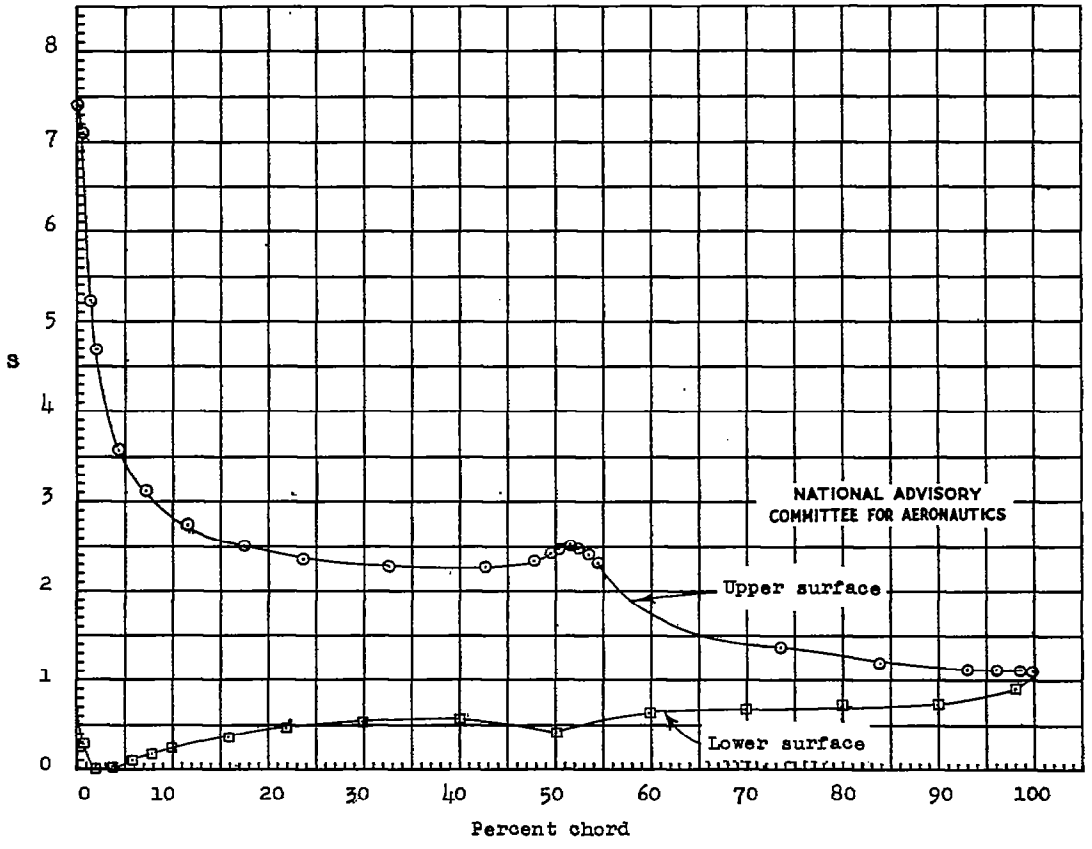

(j) $\alpha_o = 6.09^\circ$

Figure 8.- Continued.

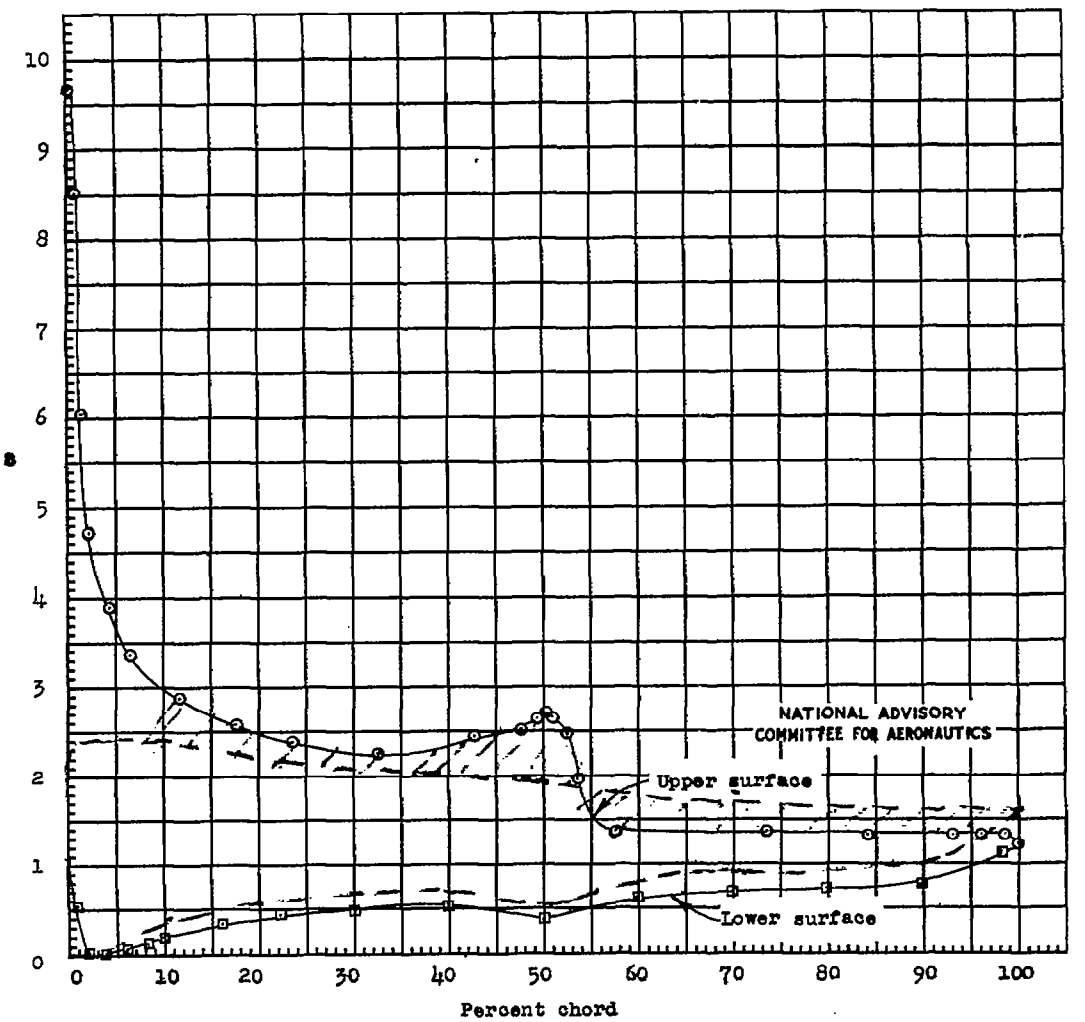

(k) $\alpha_o = 8.12^\circ$.

Figure 8.- Continued.

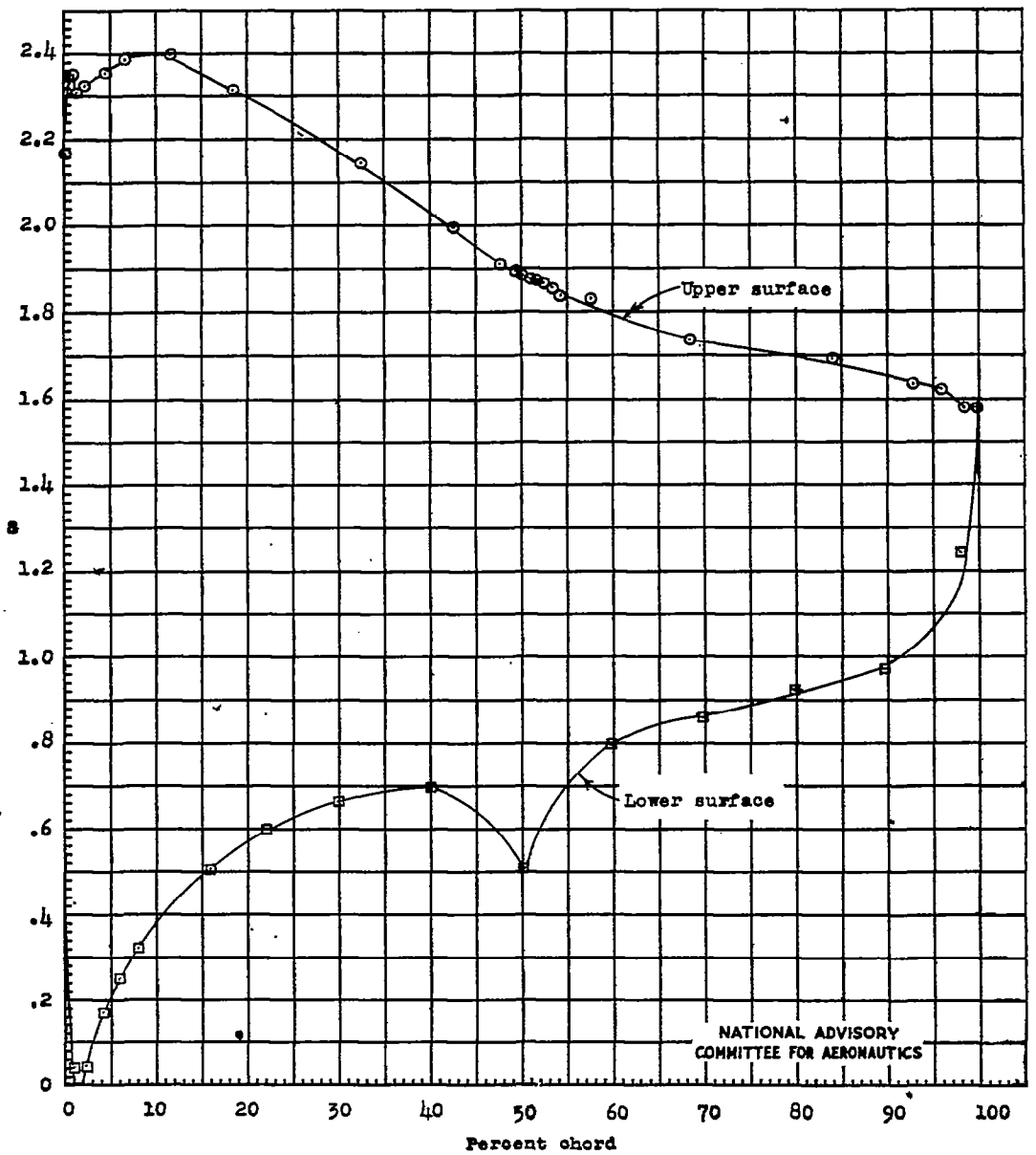

(1) $\alpha_0 = 10.15^\circ$

Figure 8.- Concluded.

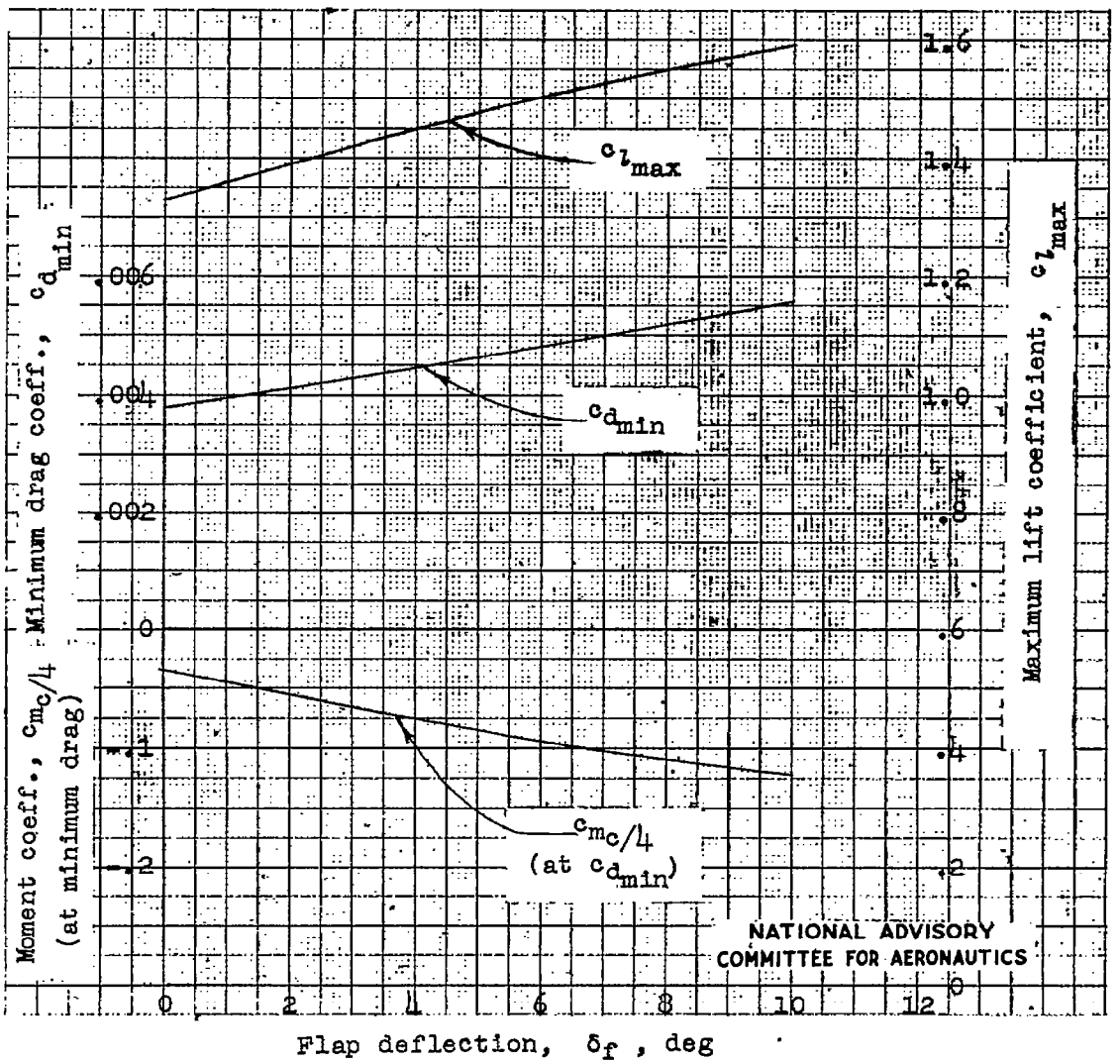

Figure 9.- Variation of section coefficients of maximum lift, minimum drag, and pitching moment at minimum drag with flap deflection for the NACA 65-210 airfoil section. $R = 6.0 \times 10^6$.

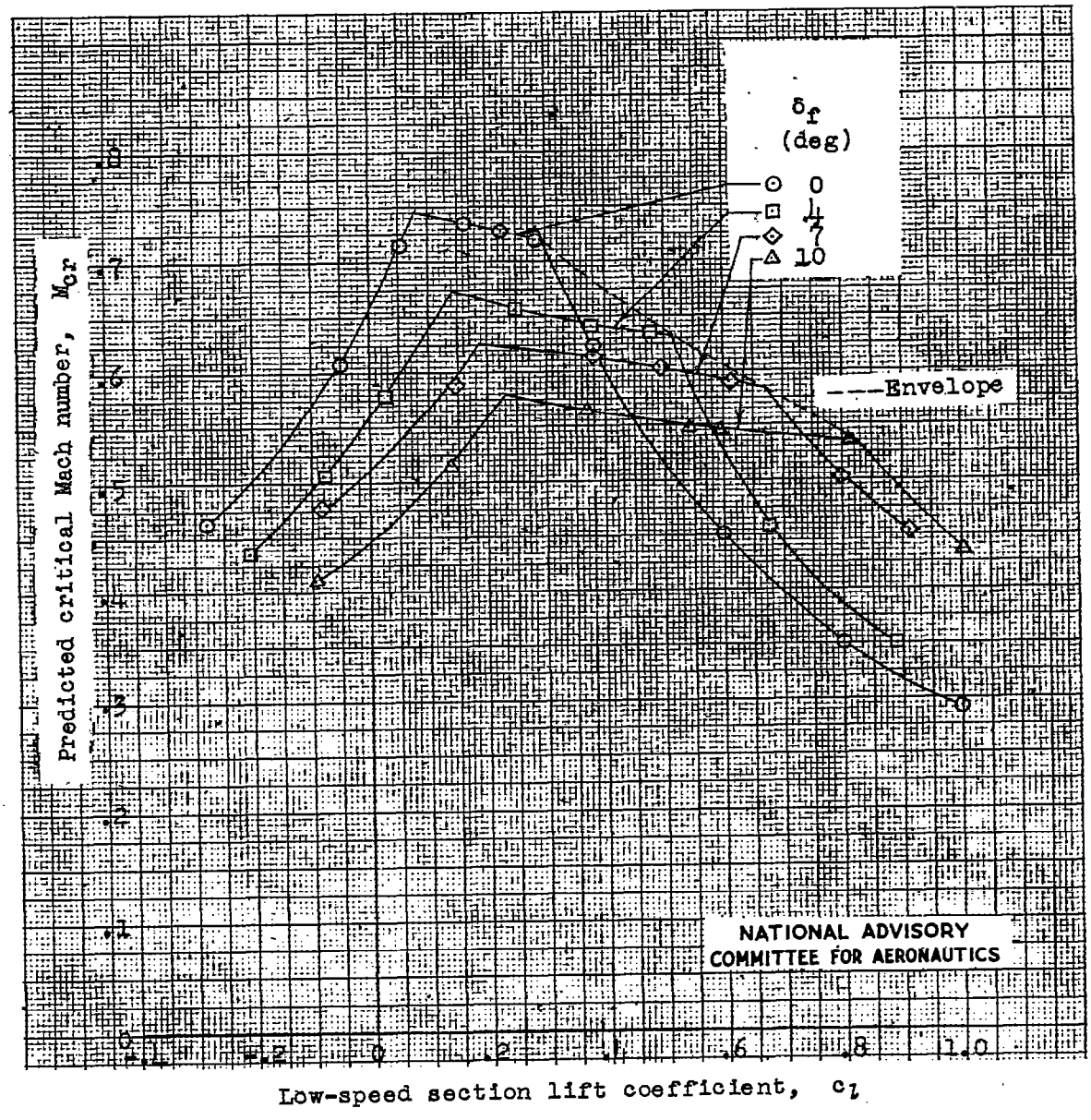

Figure 10.- Variation of predicted critical Mach number with low-speed section lift coefficient for the NACA 65-210 airfoil section at several flap deflections.

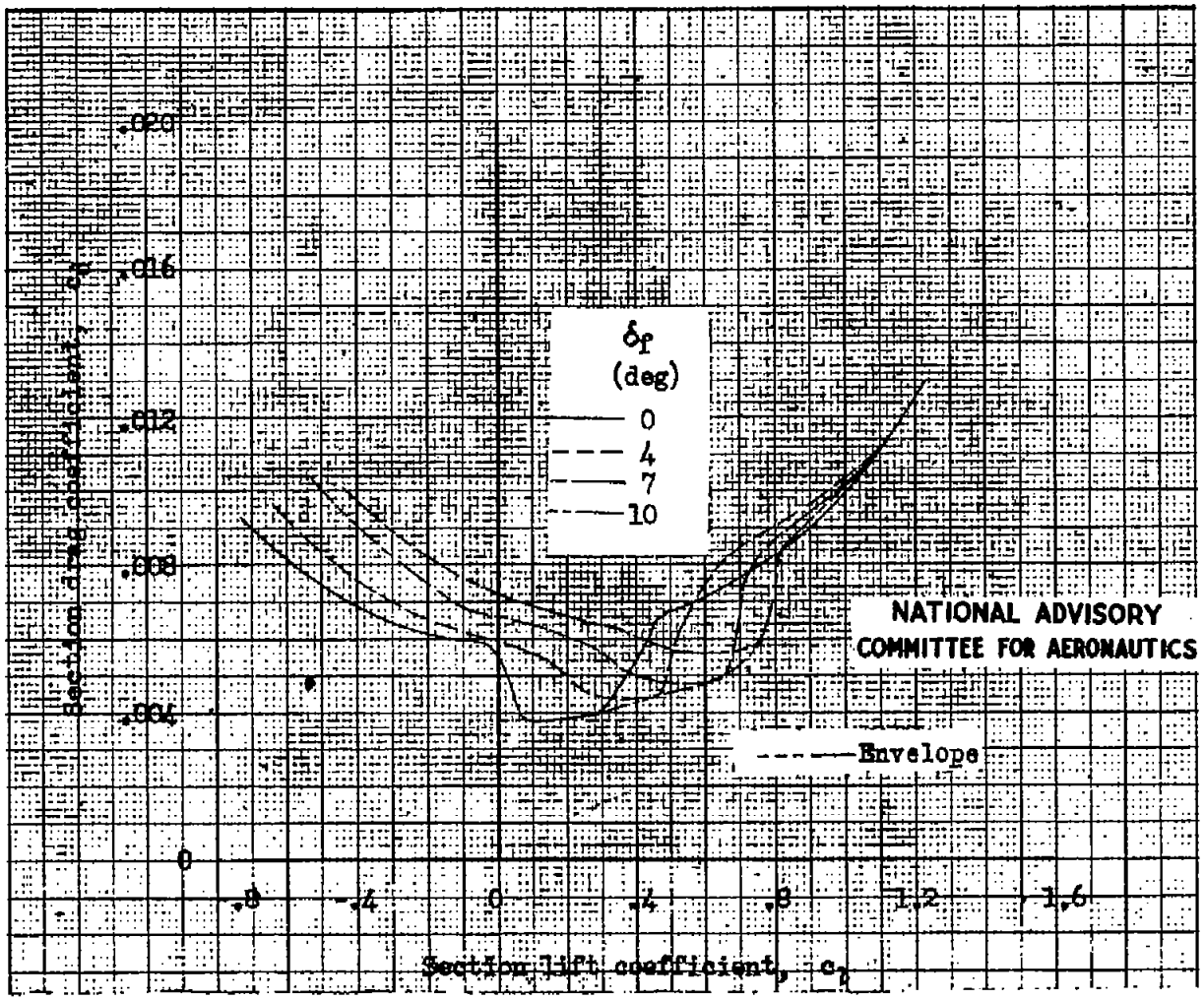

Figure 11.- Drag curves for the NACA 65-210 airfoil section at several flap deflections and their envelope. $R = 6.0 \times 10^6$.